Quiescent galaxies at the dawn of the Universe

Emiliano Merlin, INAF - OAR

Collaborators:
Paola Santini, Adriano Fontana, Marco Castellano, Flaminia Fortuni
(INAF-OAR)

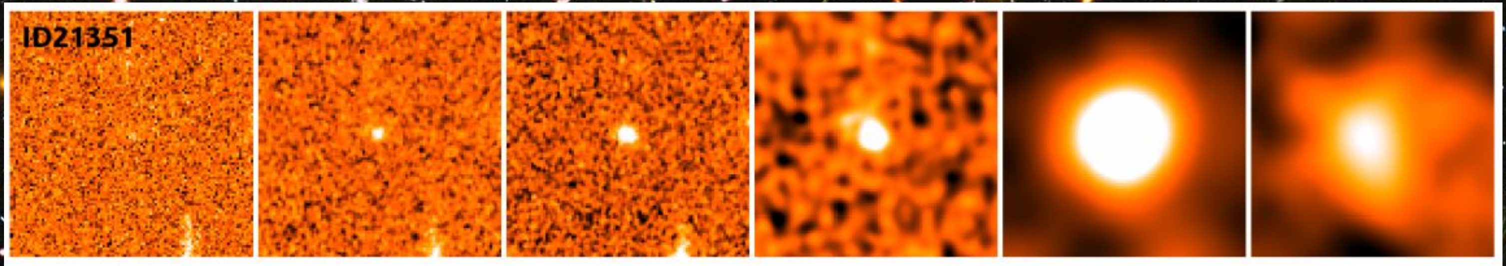

MOND40, St. Andrews, Jun 7 2023

Local galaxies come in two flavours

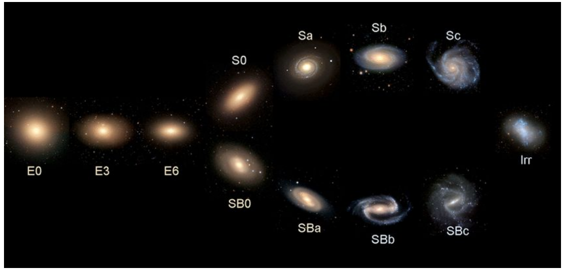

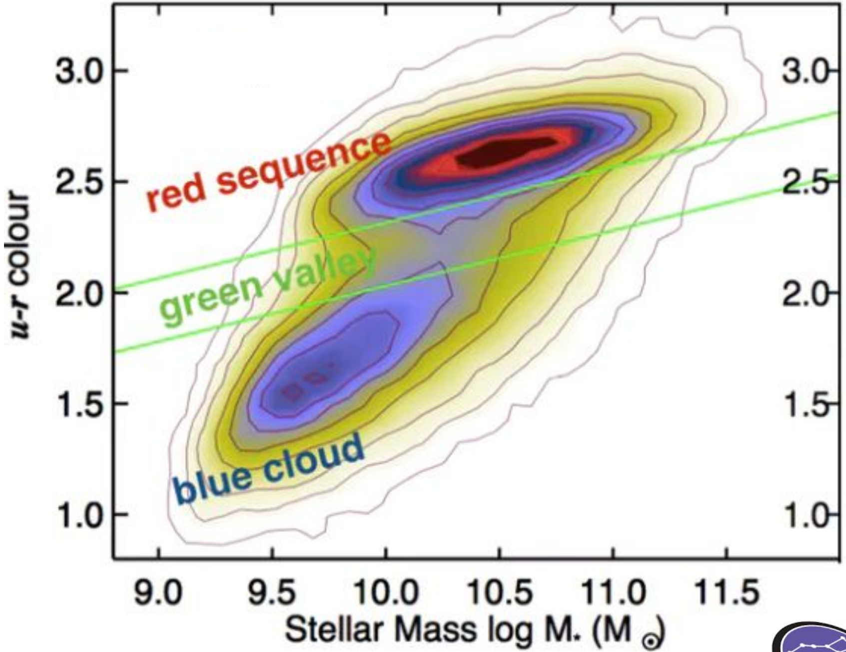

Schawinski+2014

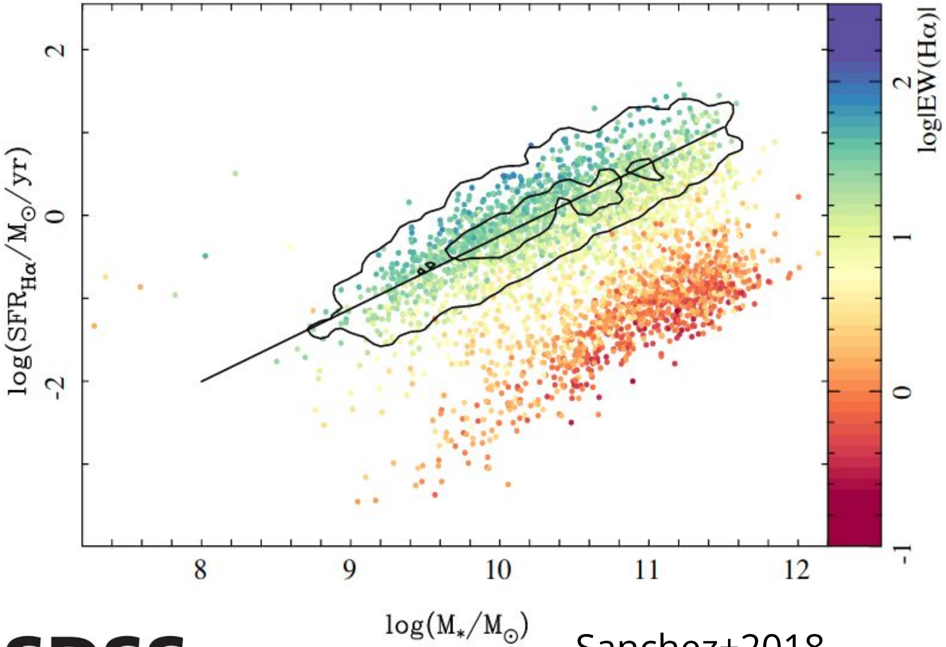

SDSS

Sanchez+2018

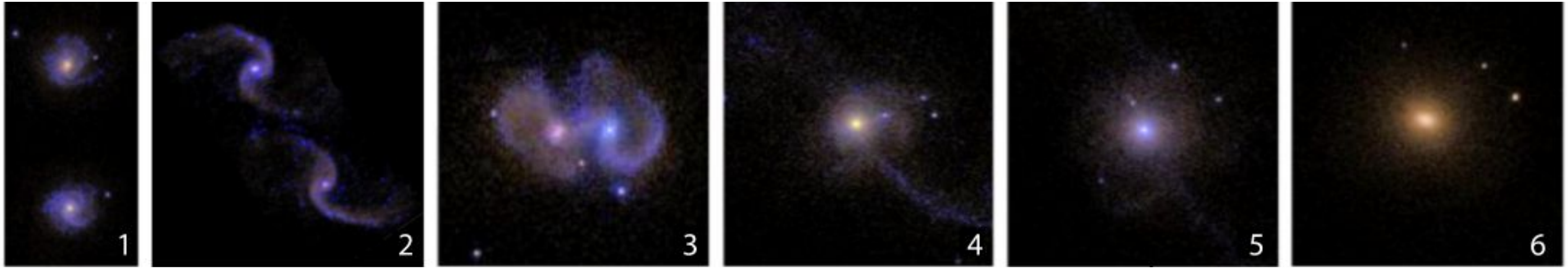

adapted from Kocevski+2015

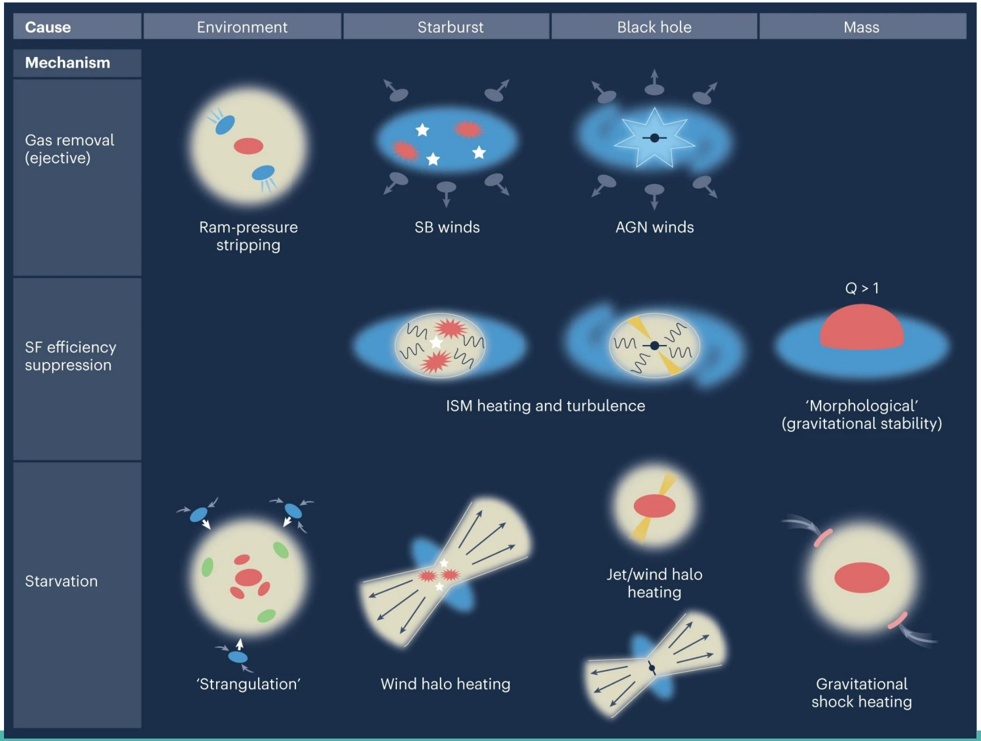

Highly non linear, local, microscopic processes

R. Maiolino

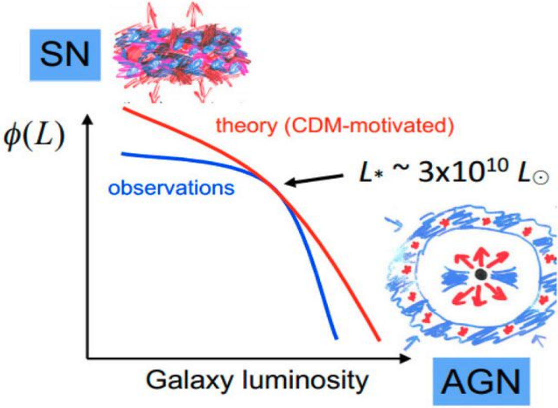

Silk+2012

Need numerical models:
SAMs or fully hydro simulations

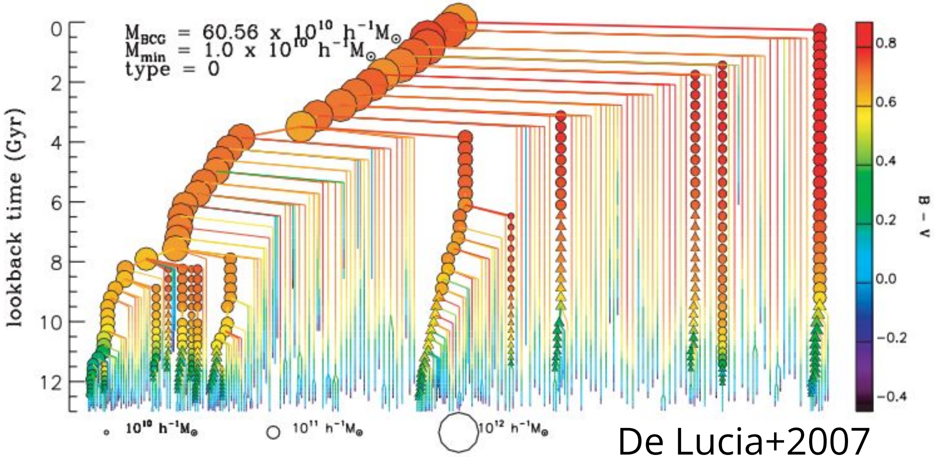

De Lucia+2007

Need numerical models:
SAMs or fully hydro simulations

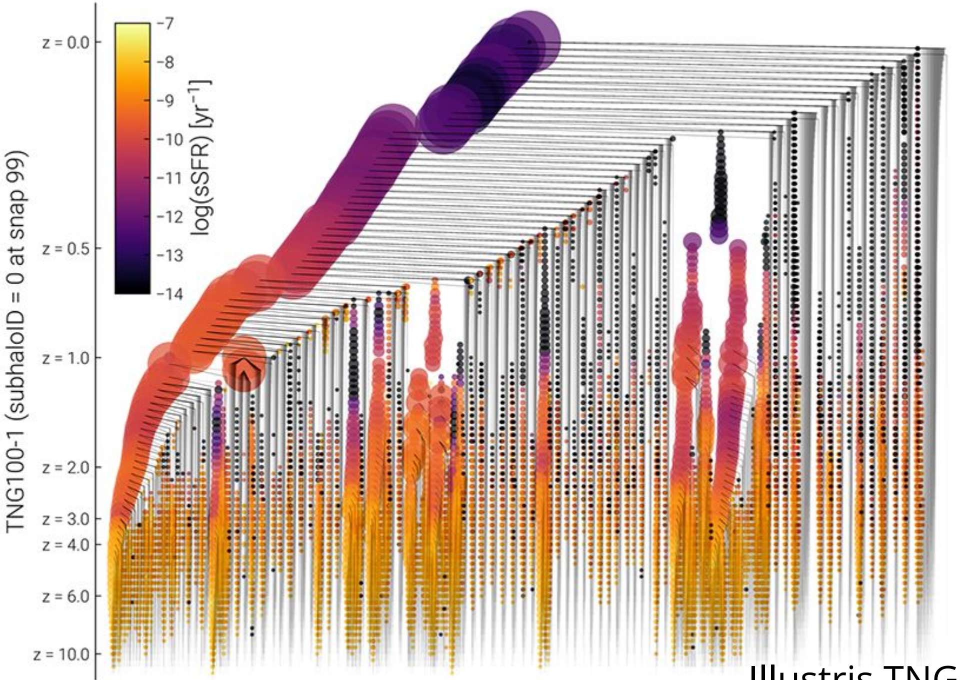

Illustris TNG 2018

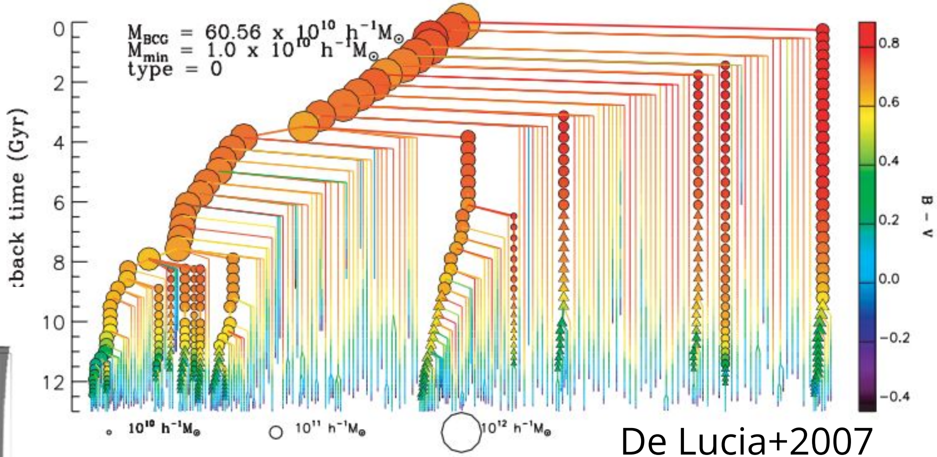

De Lucia+2007

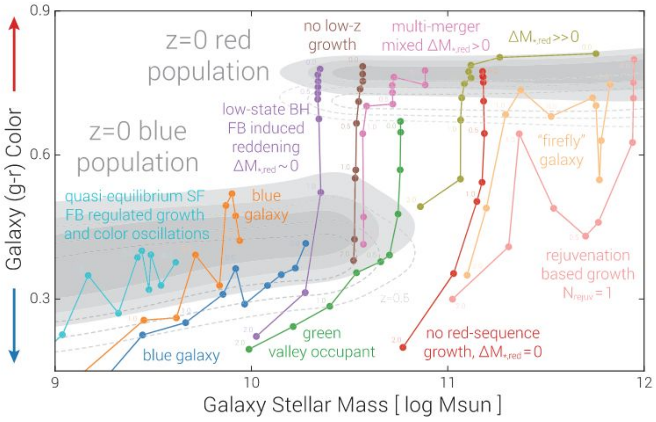

Figure 14. Schematic diagram of galaxy evolution across the colour–mass plane. The distribution of all $z = 0$ galaxies is shown by the grey contours, while the dotted lines indicate the bulk evolution of the red and blue populations to $z \simeq 0.5$, both moving downward in $(g - r)$. Eleven coloured lines show the characteristic evolutionary pathways of individual, central galaxies, from at most $z = 2$ to the present day. Although drawn from actual tracks in TNG100-1, we intend them as prototypical demonstrations of the various trajectories of central galaxies towards $z = 0$ and in particular the ways they can ascend to the red population (see the text).

“Downsizing”

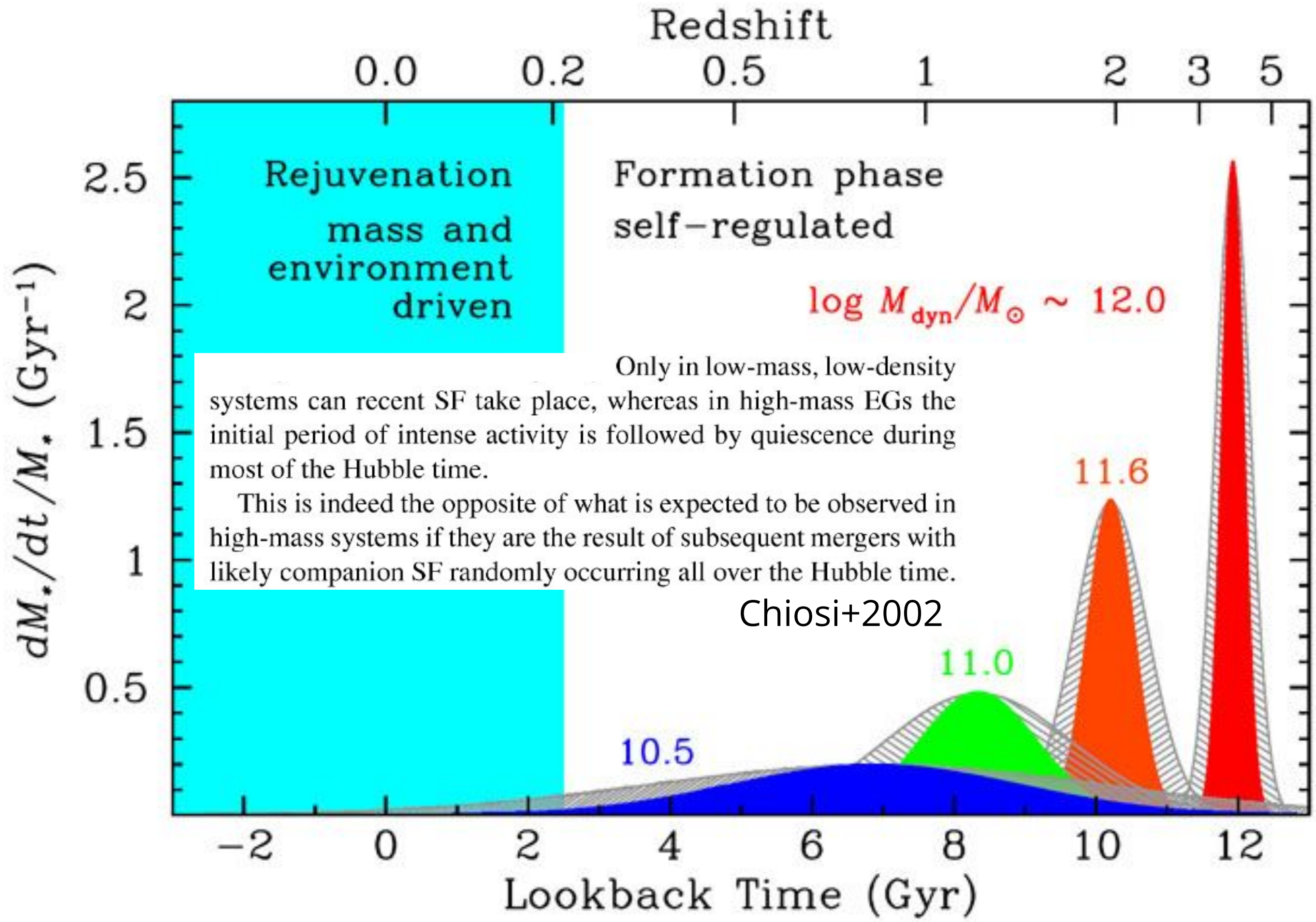

Only in low-mass, low-density systems can recent SF take place, whereas in high-mass EGs the initial period of intense activity is followed by quiescence during most of the Hubble time.

This is indeed the opposite of what is expected to be observed in high-mass systems if they are the result of subsequent mergers with likely companion SF randomly occurring all over the Hubble time.

Chiosi+2002

Evidences from chemical composition and dynamics of local ETGs

Thomas+2010

Identifying high-z passive galaxies

Observed colours

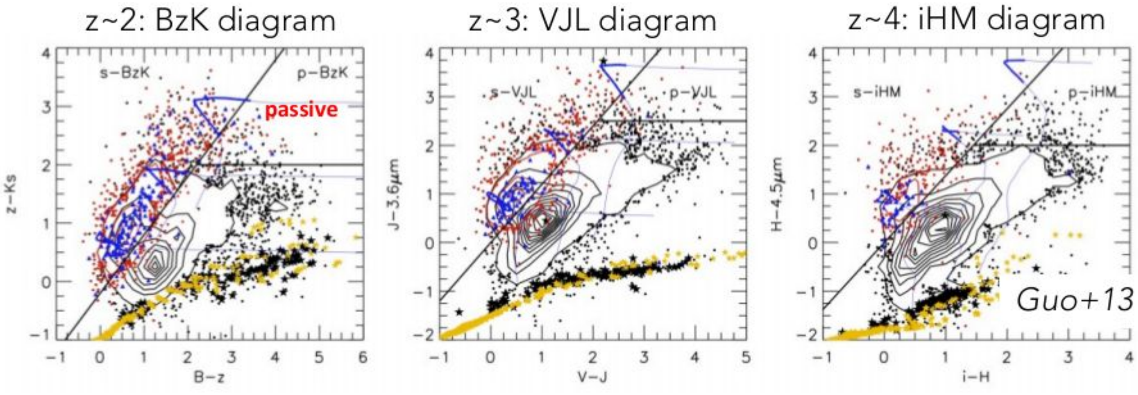

See also:
Daddi+04, Labbé+05, Wiklind+08 (JKL diagram, z>5), *Mawatari+16* (KLM diagram, z>5), …

Rest-frame colours

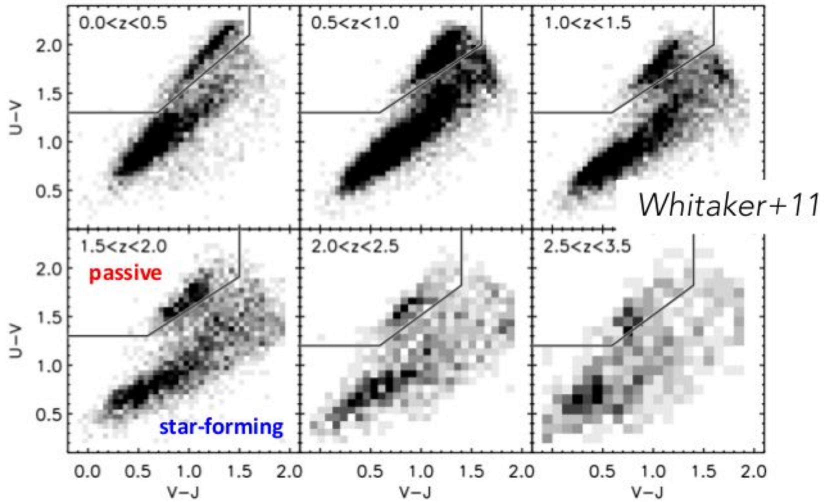

See also:
Wuyts+07, Williams+09, Patel+11, Straatman+14, Martis16, Fang+18, …. (UVJ diagram);
Arnouts+13, Ilbert+13, Davidzon+17, … (similar diagnostic diagrams)

Galaxies come in two flavours… at all epochs

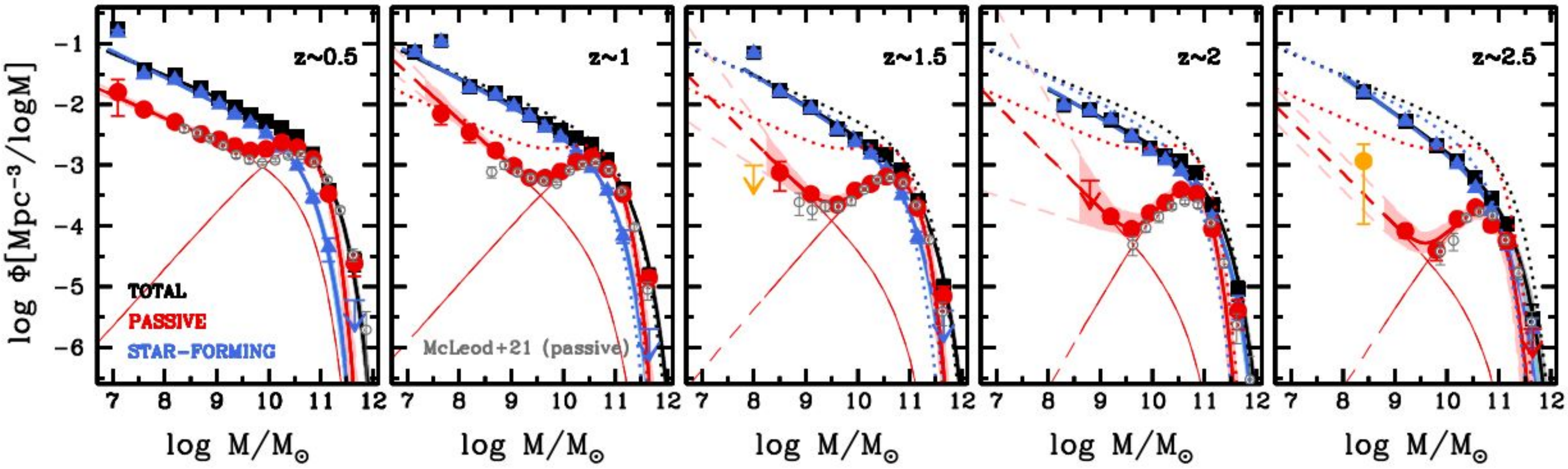

Santini+2022,
UVJ selected

z>3 passive galaxies: CANDELS

Selection based on SED fitting, assuming top-hat SFH (best hypothesis for short timescales) + probability of SF solutions

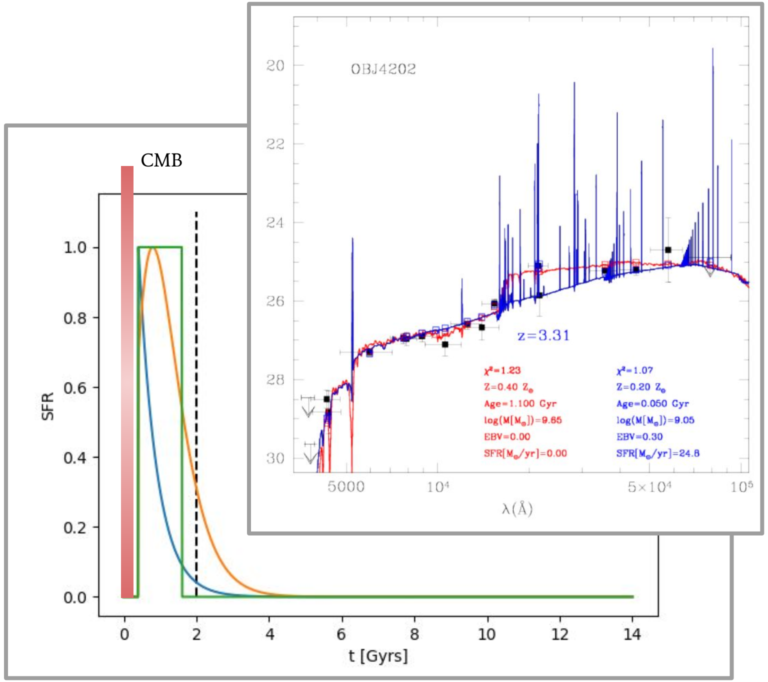

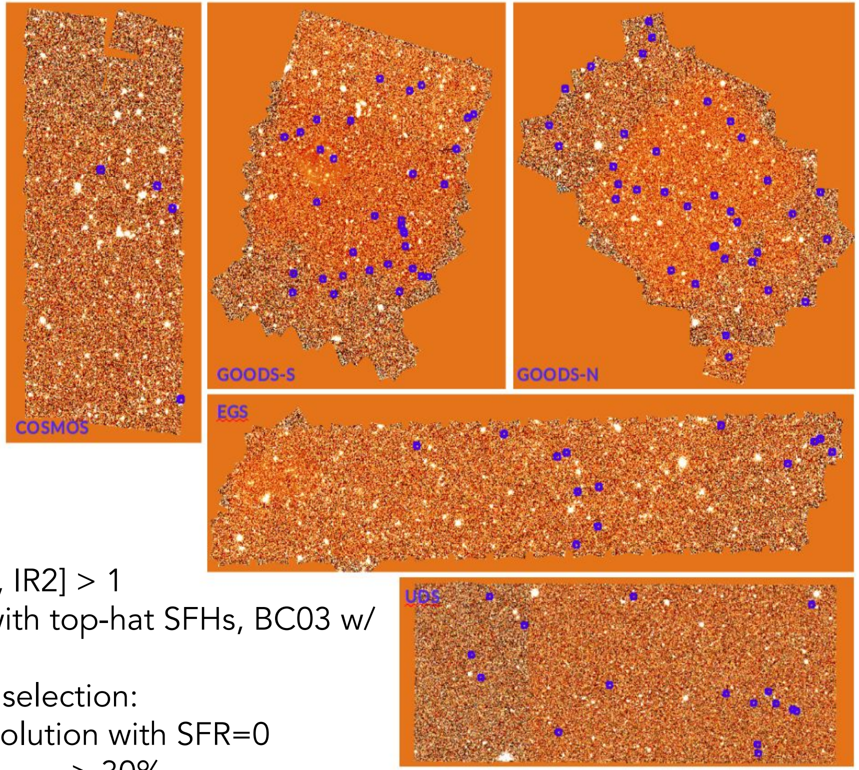

- z>3
- magH < 27
- SNR [Ks, IR1, IR2] > 1
- SED fitting with top-hat SFHs, BC03 w/ or w/o lines
- Probabilistic selection:
  - best solution with SFR=0
  - $P_{best\ (passive)}$ > 30%
  - no $P_{i\ (star\text{-}forming)}$ > 5%

Merlin+19

Red and dead CANDELS: massive passive galaxies at the dawn of the Universe

E. Merlin,[1★] F. Fortuni,[1] M. Torelli,[1] P. Santini,[1] M. Castellano,[1] A. Fontana,[1] A. Grazian,[2] L. Pentericci,[1] S. Pilo[1] and K. B. Schmidt[3]
[1]INAF - Osservatorio Astronomico di Roma, via Frascati 33, I-00078 Monte Porzio Catone (RM), Italy
[2]INAF - Osservatorio Astronomico di Padova, Vicolo Osservatorio 5, I-35122 Padova, Italy
[3]Leibniz-Institut für Astrophysik Potsdam (AIP), An der Sternwarte 16, I-14482 Potsdam, Germany

Accepted 2019 September 11. Received 2019 August 26; in original form 2019 May 22

Field/Sample	Total	$z > 3$	$S/N_{z>3} > 1$	Reference	Lines
COSMOS	38 671	3778	1525	4	2
EGS	41 457	4830	1775	13	5
GOODS-N	35 445	3953	1793	36	11
GOODS-S	34 930	5029	2884	33	13
UDS	35 932	4018	2540	16	9
All fields	186 435	21 608	10 517	102	40

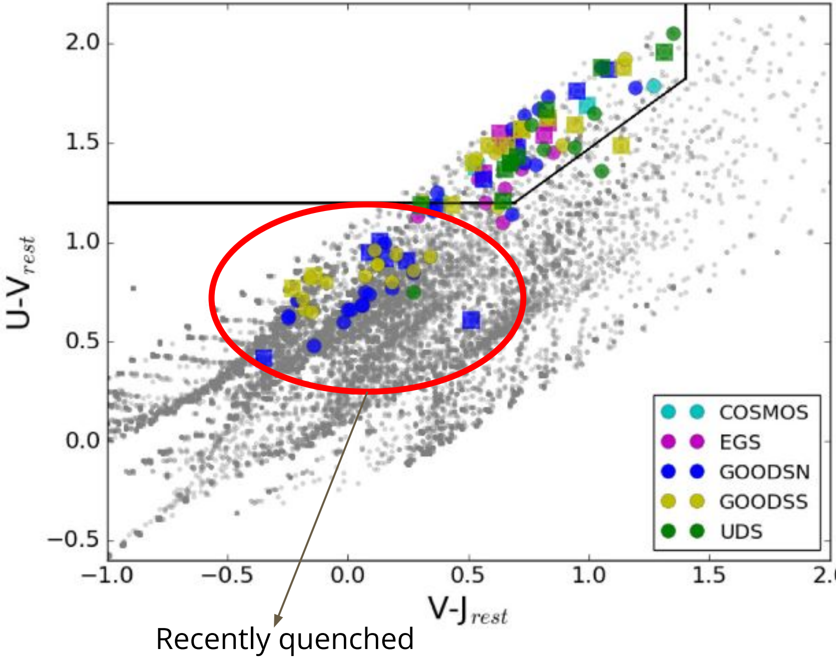

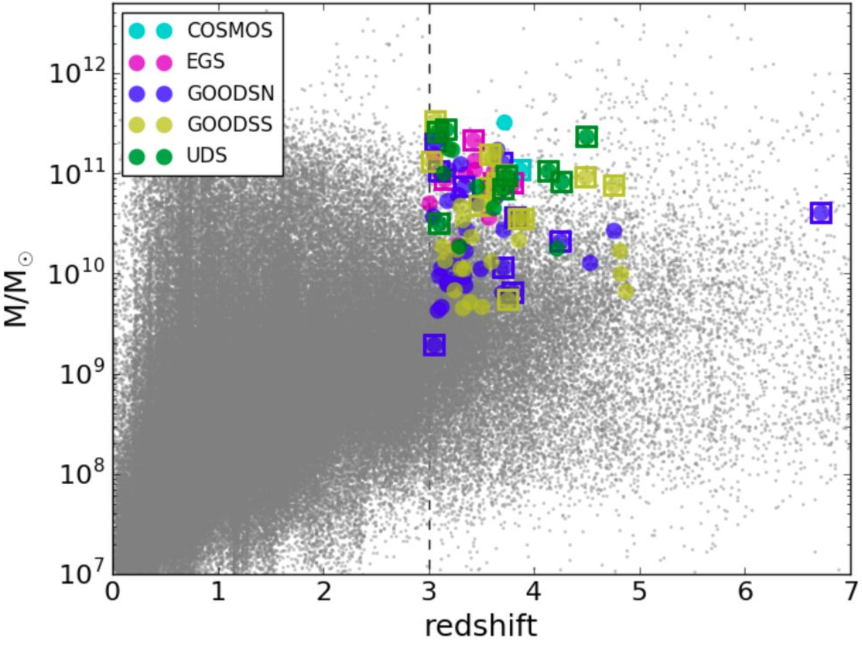

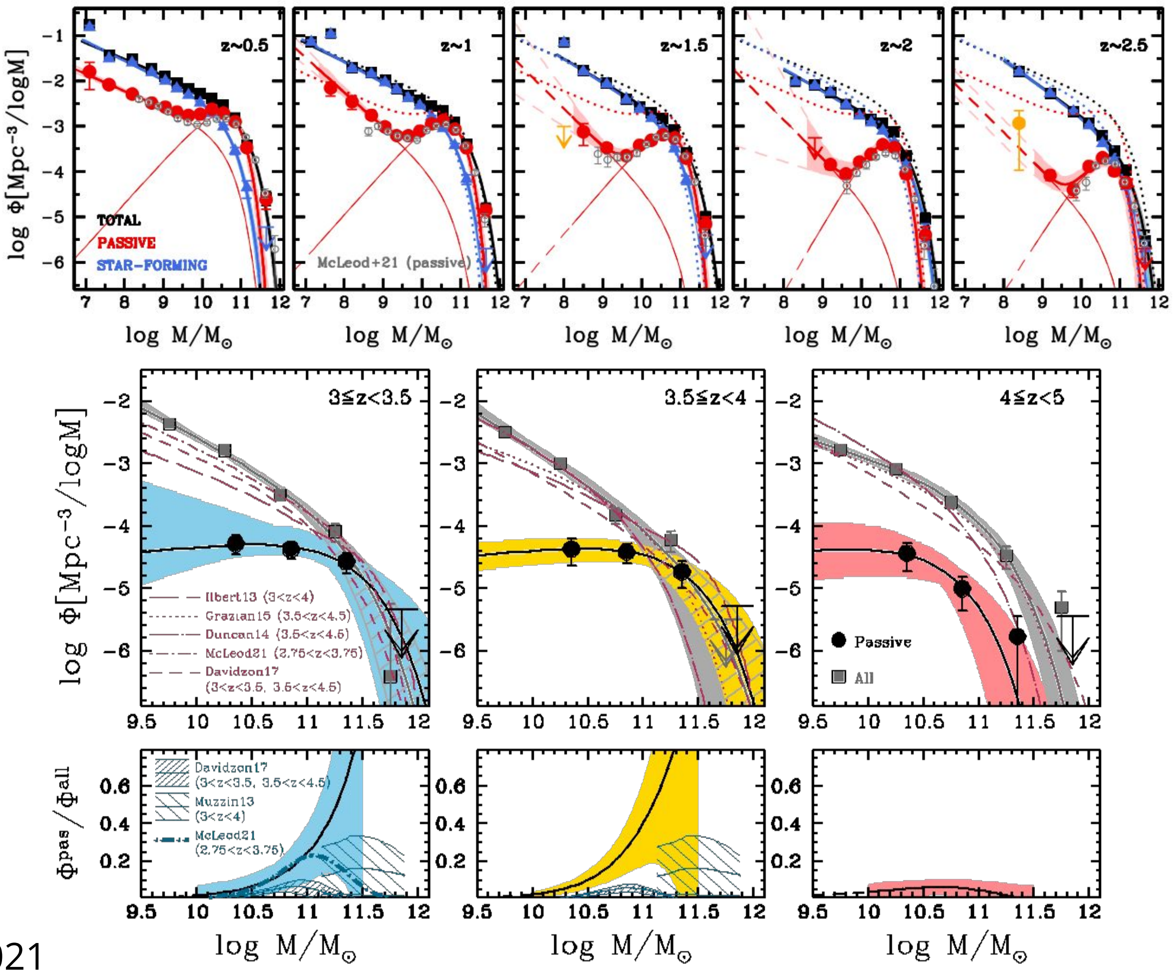

Santini+2021

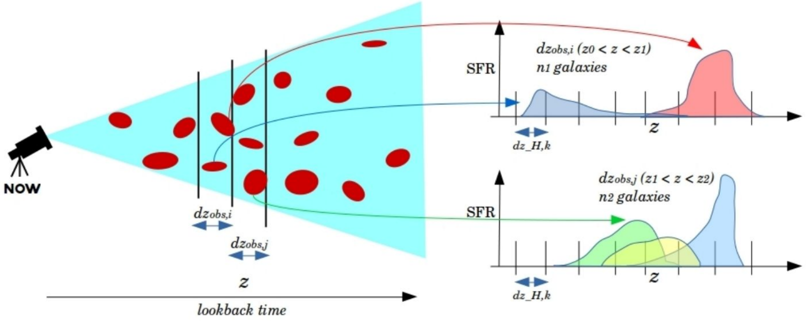

We are fairly consistent with the observed SFRDs at z<5, but predict a ~constant SFRD up to z~10

Our Red&Deads are ~0.5% of all *z*>3 galaxies, but provide ~5-10% of cosmic SFRD at 3<z<8

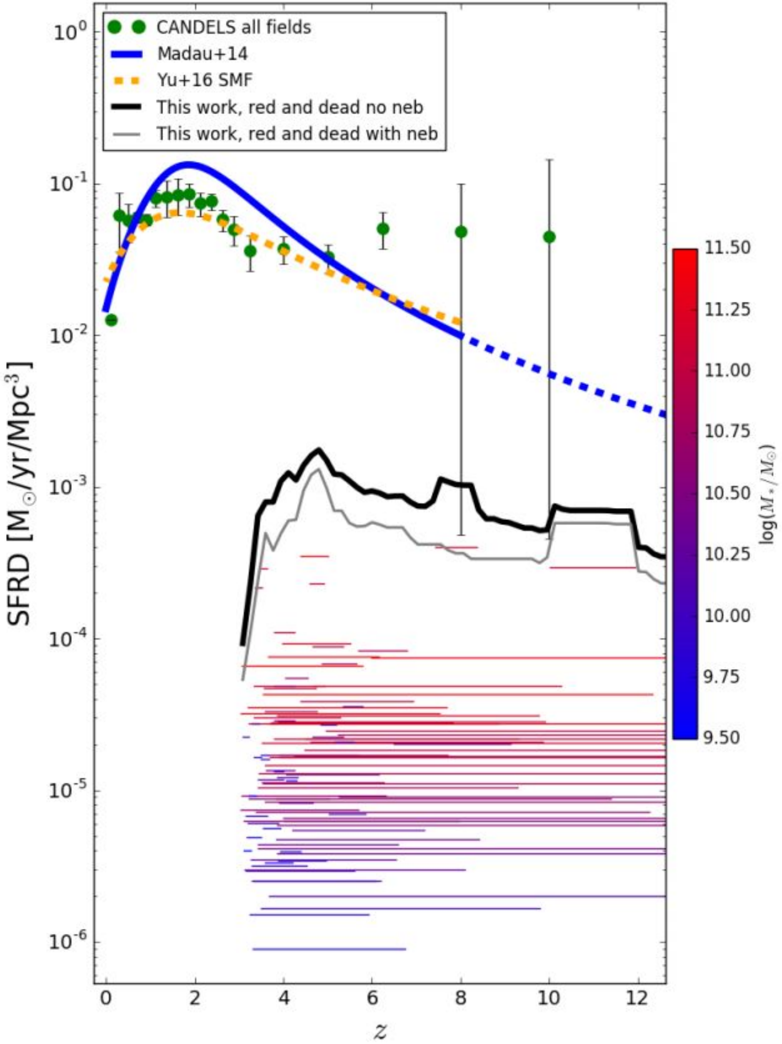

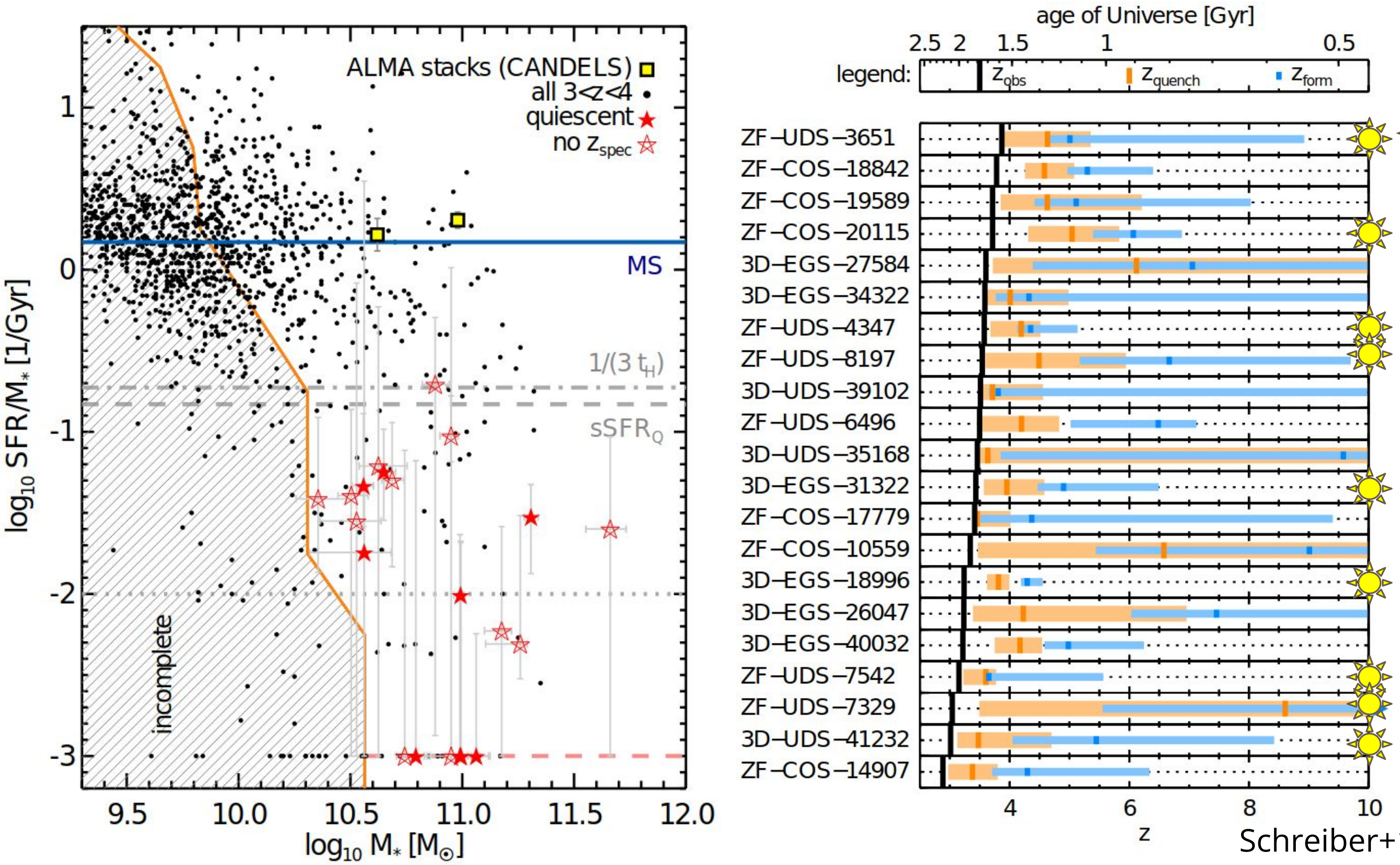

EM+19 sample

Schreiber+18

JWST

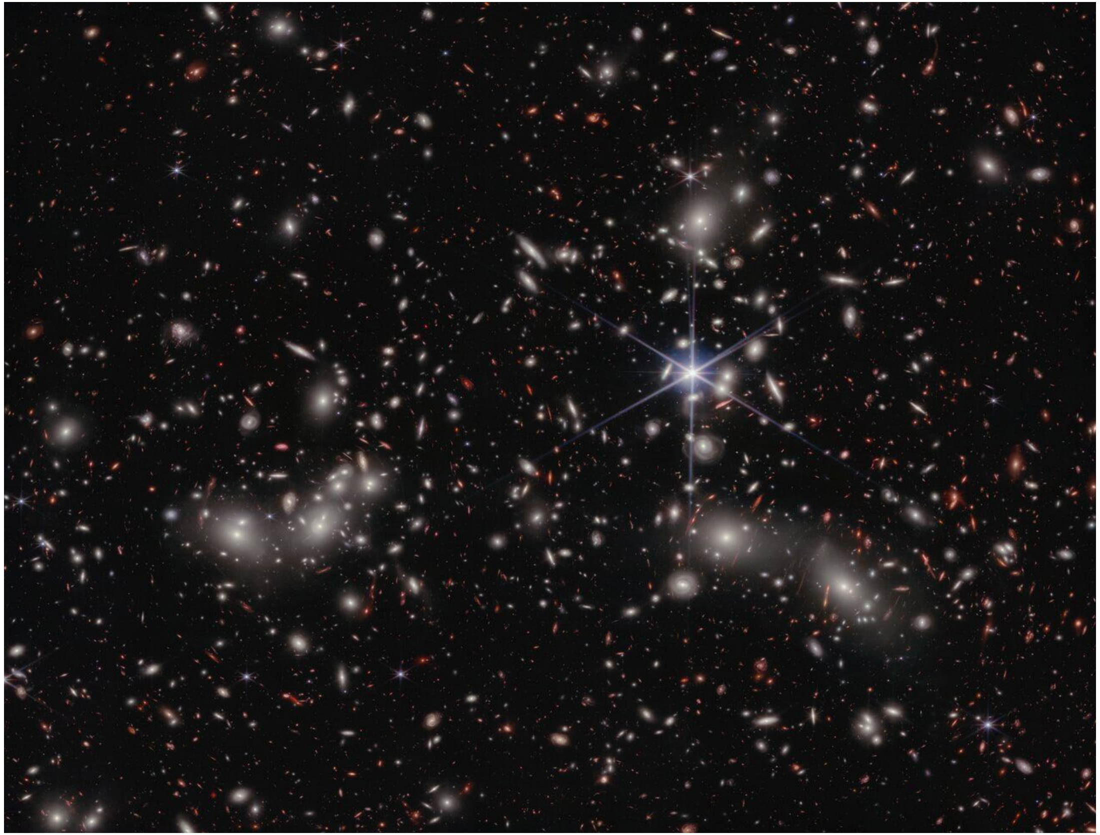

The Astrophysical Journal Letters, 938:L14 (8pp), 2022 October 20 https://doi.org/10.3847/2041-8213/ac8f93
© 2022. The Author(s). Published by the American Astronomical Society.
OPEN ACCESS

CrossMark

Early Results from GLASS-JWST. II. NIRCam Extragalactic Imaging and Photometric Catalog

Emiliano Merlin[1], Andrea Bonchi[2], Diego Paris[1], Davide Belfiori[1], Adriano Fontana[1], Marco Castellano[1], Mario Nonino[3], Gianluca Polenta[2], Paola Santini[1], Lilan Yang[4], Karl Glazebrook[5], Tommaso Treu[6], Guido Roberts-Borsani[6], Michele Trenti[7,8], Simon Birrer[9,10,11], Gabriel Brammer[12,13], Claudio Grillo[14,15], Antonello Calabrò[1], Danilo Marchesini[16], Charlotte Mason[12,17], Amata Mercurio[18], Takahiro Morishita[19], Victoria Strait[12,17], Kristan Boyett[7,8], Nicha Leethochawalit[7,8,20], Themiya Nanayakkara[21], Benedetta Vulcani[22], Marusa Bradac[23,24], and Xin Wang[25]

The Astrophysical Journal Letters, 938:L15 (9pp), 2022 October 20 https://doi.org/10.3847/2041-8213/ac94d0
© 2022. The Author(s). Published by the American Astronomical Society.
OPEN ACCESS

CrossMark

Early Results from GLASS-JWST. III. Galaxy Candidates at $z \sim 9$–15*

Marco Castellano[1], Adriano Fontana[1], Tommaso Treu[2], Paola Santini[1], Emiliano Merlin[1], Nicha Leethochawalit[3,4,5], Michele Trenti[3,4], Eros Vanzella[6], Uros Mestric[6], Andrea Bonchi[7], Davide Belfiori[1], Mario Nonino[8], Diego Paris[1], Gianluca Polenta[7], Guido Roberts-Borsani[2], Kristan Boyett[3,4], Maruša Bradač[9,10], Antonello Calabrò[1], Karl Glazebrook[11], Claudio Grillo[12,13], Sara Mascia[1], Charlotte Mason[14,15], Amata Mercurio[16], Takahiro Morishita[17], Themiya Nanayakkara[11], Laura Pentericci[1], Piero Rosati[18,19], Benedetta Vulcani[20], Xin Wang[21], and Lilan Yang[22]

CrossMark

Early Results from GLASS-JWST. XI. Stellar Masses and Mass-to-light Ratio of $z > 7$ Galaxies

P. Santini[1], A. Fontana[1], M. Castellano[1], N. Leethochawalit[2,3,4], M. Trenti[2,3], T. Treu[5], D. Belfiori[1], S. Birrer[6,7], A. Bonchi[1,8], E. Merlin[1], C. Mason[9,10], T. Morishita[11], M. Nonino[12], D. Paris[1], G. Polenta[8], P. Rosati[13,14], L. Yang[15], K. Boyett[2], M. Bradac[16,17], A. Calabrò[1], A. Dressler[18], K. Glazebrook[19], D. Marchesini[20], S. Mascia[1], T. Nanayakkara[19], L. Pentericci[1], G. Roberts-Borsani[5], C. Scarlata[21], B. Vulcani[22], and Xin Wang[23]

The GLASS-JWST Early Release Science Program. II. Stage I release of NIRCam imaging and catalogs in the Abell 2744 region.

Diego Paris,[1] Emiliano Merlin,[1] Adriano Fontana,[1] Andrea Bonchi,[2,1] Gabriel Brammer,[3,4] Matteo Correnti,[2,1] Tommaso Treu,[5] Kristan Boyett,[6,7] Antonello Calabrò,[1] Marco Castellano,[1] Wenlei Chen,[8] Lilan Yang,[9] K. Glazebrook,[10] Patrick Kelly,[8] Anton M. Koekemoer,[11] Nicha Leethochawalit,[12] Sara Mascia,[1] Charlotte Mason,[3,4] Takahiro Morishita,[13] Mario Nonino,[14] Laura Pentericci,[1] Gianluca Polenta,[2] Guido Roberts-Borsani,[5] Paola Santini,[1] Michele Trenti,[6,7] Eros Vanzella,[15] Benedetta Vulcani,[16] Rogier A. Windhorst,[17] Themiya Nanayakkara,[10] and Xin Wang[18,19,20]

CrossMark

Early Results from GLASS-JWST. XIX. A High Density of Bright Galaxies at $z \approx 10$ in the A2744 Region

Marco Castellano[1], Adriano Fontana[1], Tommaso Treu[2], Emiliano Merlin[1], Paola Santini[1], Pietro Bergamini[3,4], Claudio Grillo[3,5], Piero Rosati[4,6], Ana Acebron[3,5], Nicha Leethochawalit[7], Diego Paris[1], Andrea Bonchi[8], Davide Belfiori[1], Antonello Calabrò[1], Matteo Correnti[1,8], Mario Nonino[9], Gianluca Polenta[8], Michele Trenti[10,11], Kristan Boyett[10,11], G. Brammer[12,13], Tom Broadhurst[14,15,16], Gabriel B. Caminha[17,18], Wenlei Chen[19], Alexei V. Filippenko[20], Flaminia Fortuni[1], Karl Glazebrook[21], Sara Mascia[1], Charlotte A. Mason[22,23], Nicola Menci[1], Massimo Meneghetti[4,24], Amata Mercurio[25,26], Benjamin Metha[2,10,11], Takahiro Morishita[27], Themiya Nanayakkara[21], Laura Pentericci[1], Guido Roberts-Borsani[2], Namrata Roy[28], Eros Vanzella[4], Benedetta Vulcani[29], Lilan Yang[30], and Xin Wang[31,32,33]

astrodeep.eu

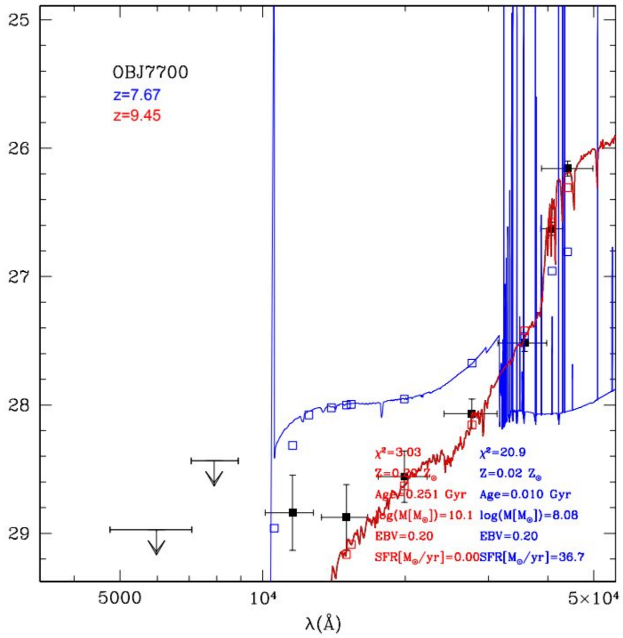

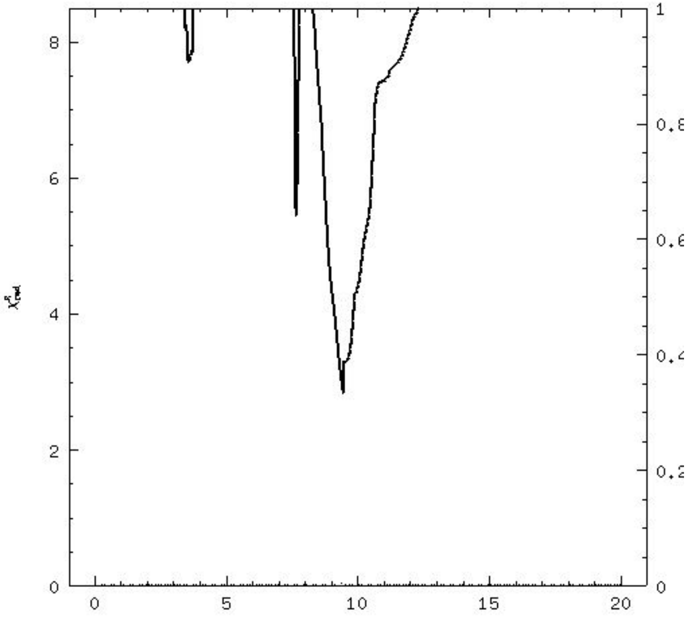

A candidate at z=9.45…

But poor optical data

HST ACS

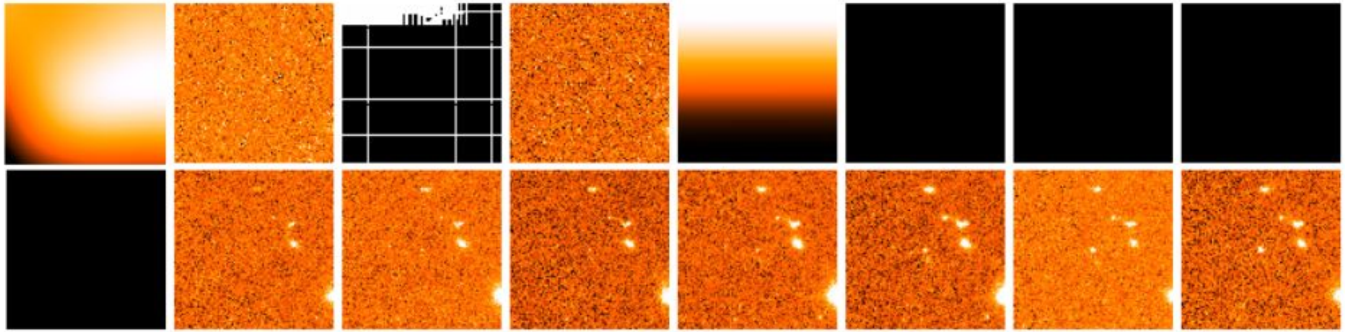

HST WFC3

JWST NIRCam

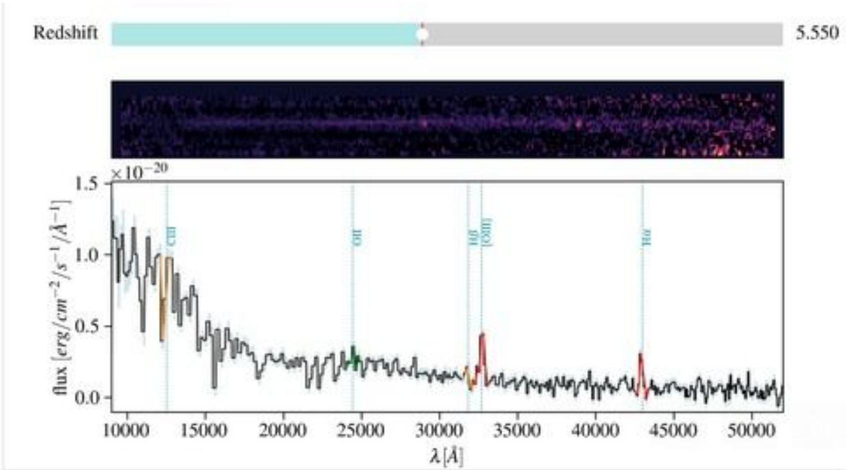

OBJ: 40202, initial z = 3.728

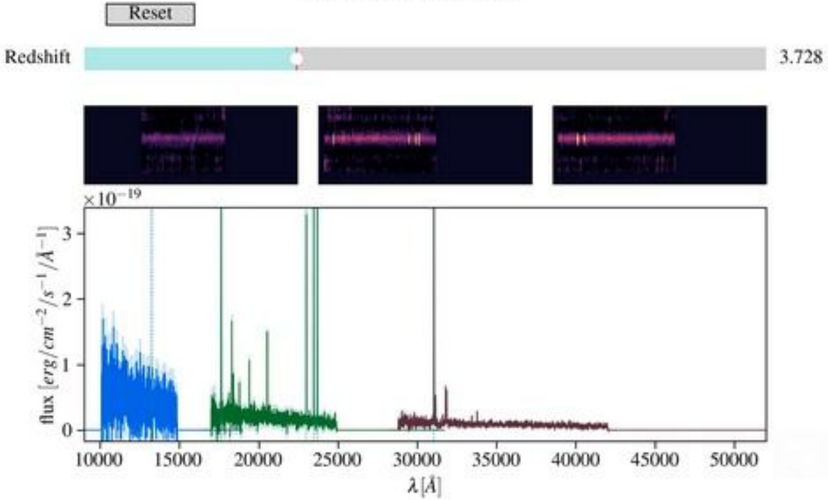

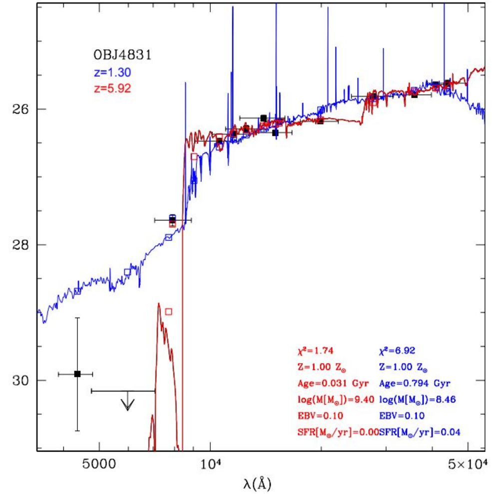

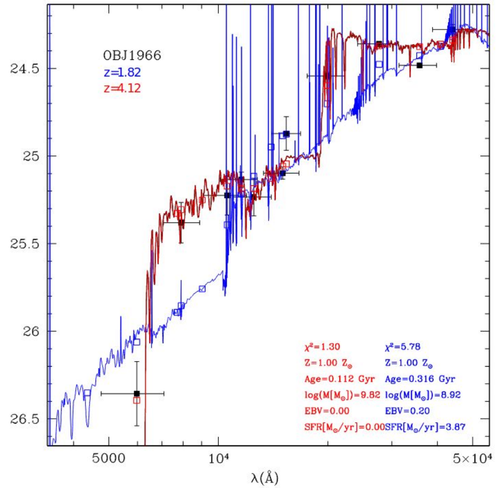

Looking for quiescent sources at such early epochs is extremely challenging

- very short timescales
- might be only temporarily quenched, although the more massive, the more likely to be red & dead

“If $\log_{10}(M_*/M)\sim11$ galaxies already exist by $6<z<10$, these must equally rapidly quench, and remain quenched, to avoid becoming too massive to be accommodated by the lower-redshift galaxy stellar mass function (e.g. McLeod et al. 2021). This suggests massive quiescent galaxies at least as early as $z\sim6$” (Carnall+2023)

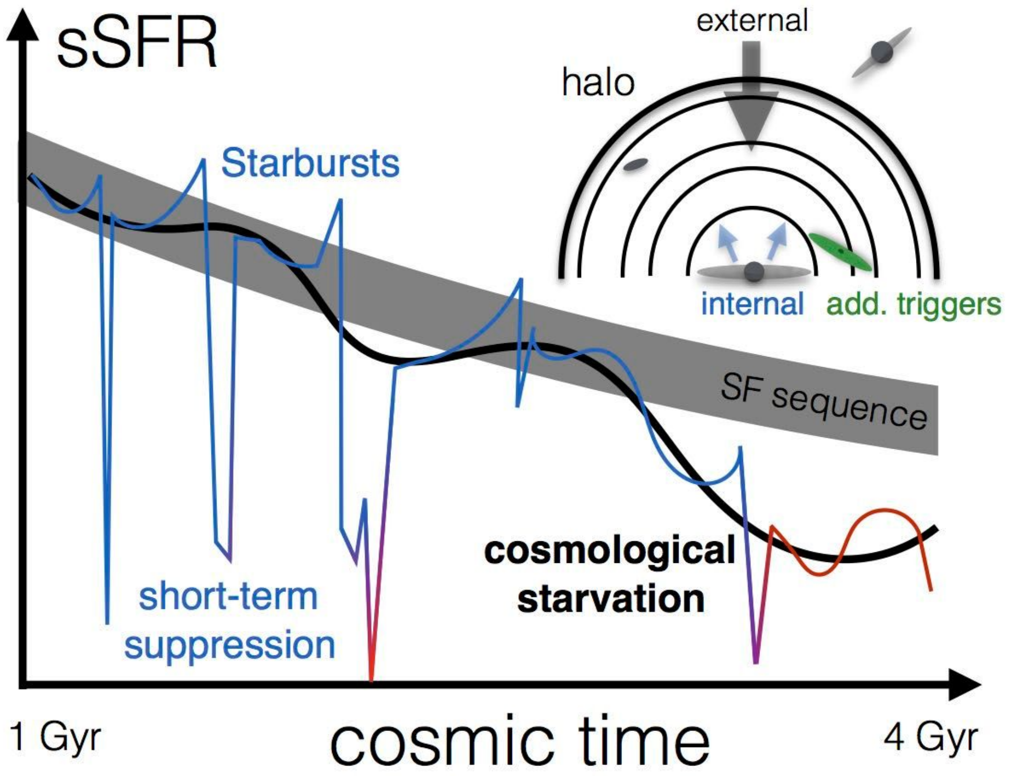

R. Feldmann

Breathing (a.k.a. re-juvenation)

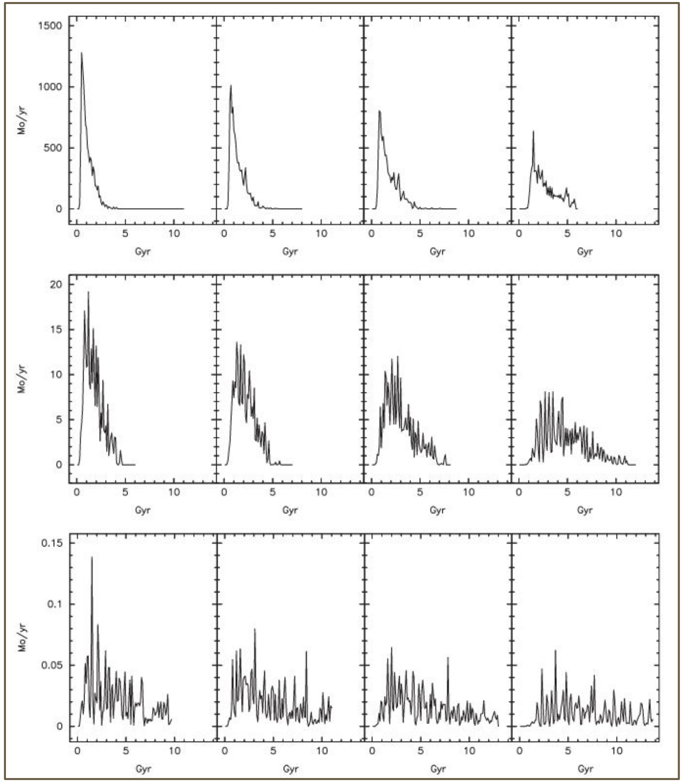

EM, Chiosi 2012

Can explain wrong candidates: Balmer break is created by the older populations

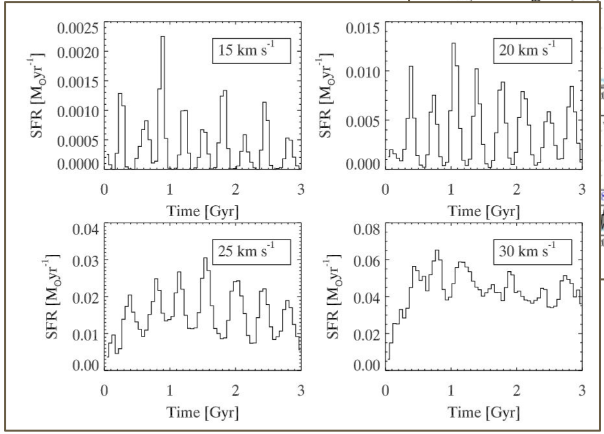

Stinson+2007

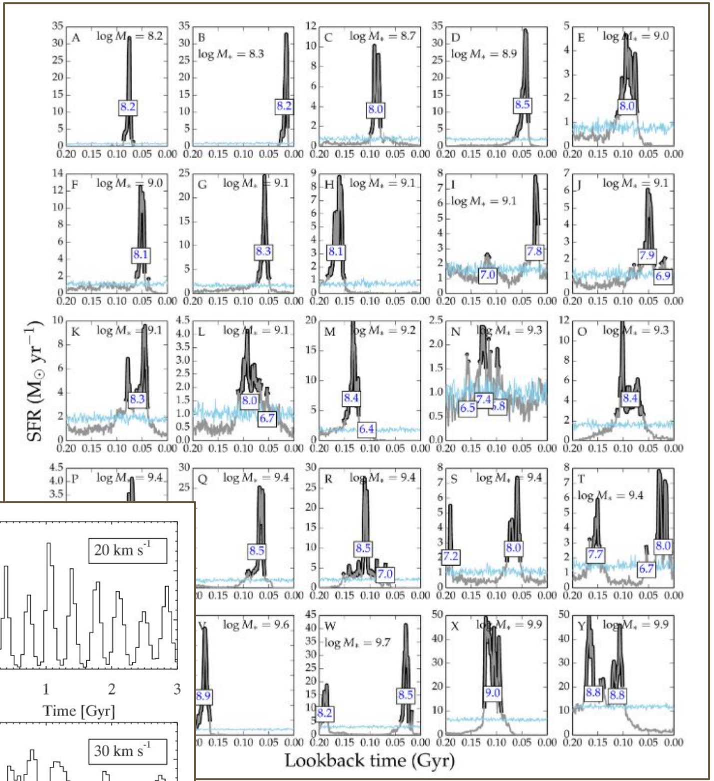

Sparre+2016 FIRE

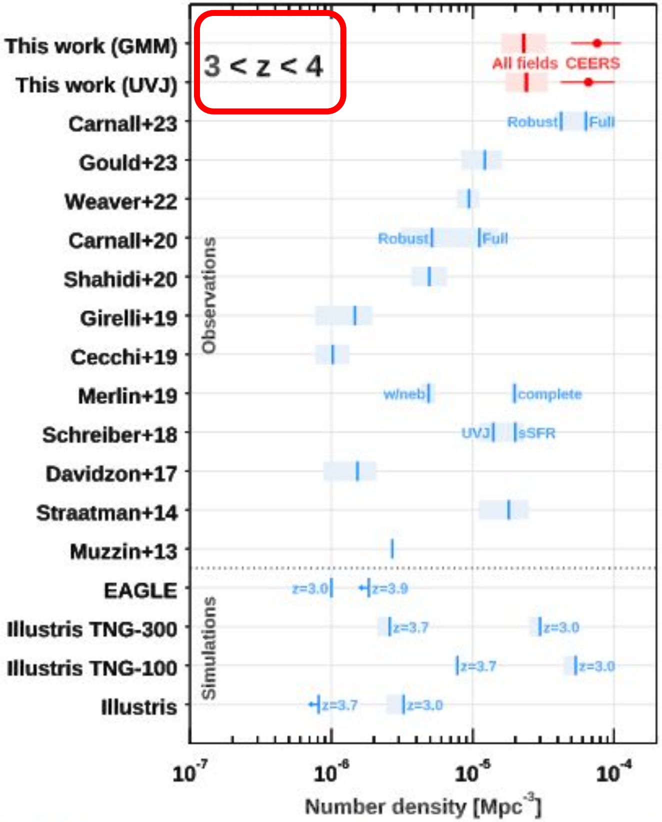

Figure 5. Comoving number densities of massive QGs in the literature. The values have been homogenized in terms of redshift interval ($3 \lesssim z \lesssim 4$) and lower mass cut ($\log(M_*/M_\odot) \gtrsim 10.6$, similar IMF) to the largest possible extent. The uncertainties do not include the contribution of cosmic variance. The estimates are reported in Table 4 in Appendix D, along with complementary information.

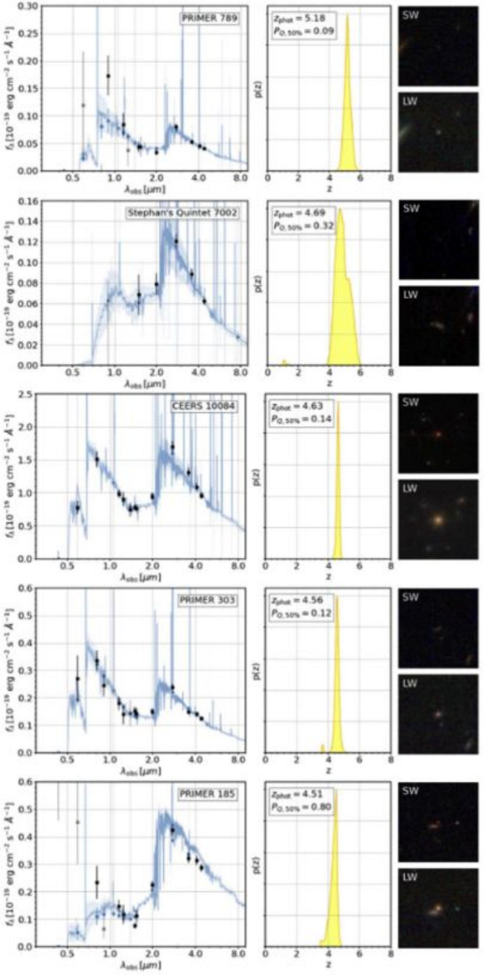

Figure 6. Robust $z > 4.5$ quiescent candidates. Left column: SEDs. Black

Field
CEERS
Stephan's Quintet
PRIMER
NEP
J1235
GLASS
Sunrise
SMACS 0723
SGAS 1723
SPT 0418
SPT 2147[c]

A robust sample of ~80 candidate quiescent and quenching galaxies at 3 < z < 5, color selected

Valentino+2023

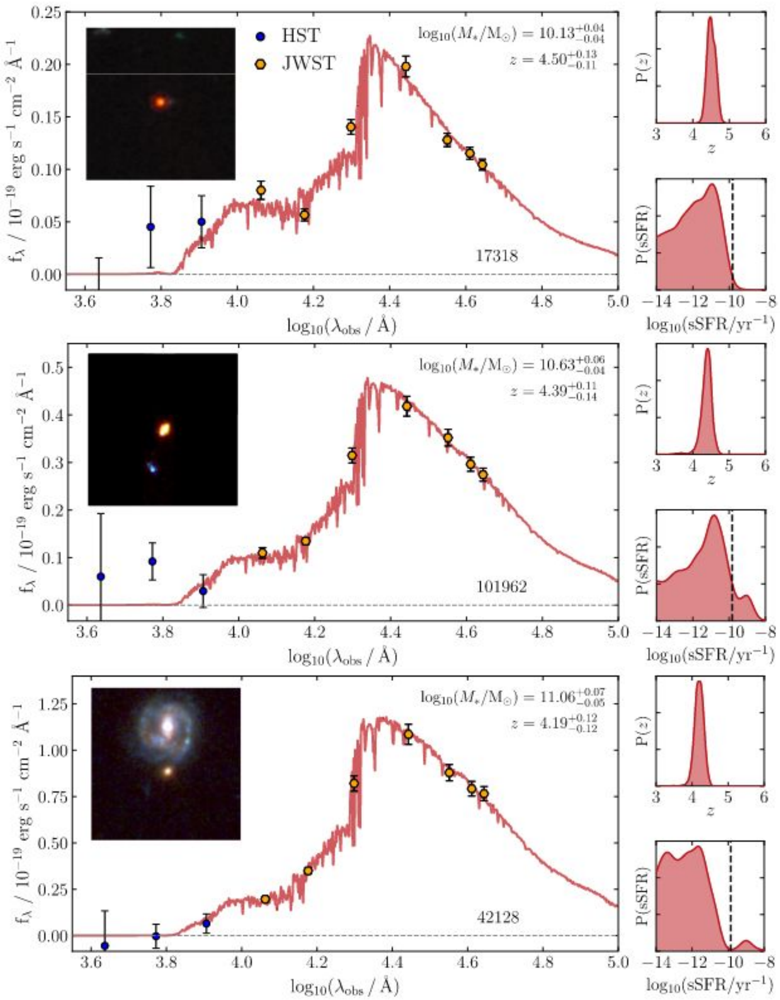

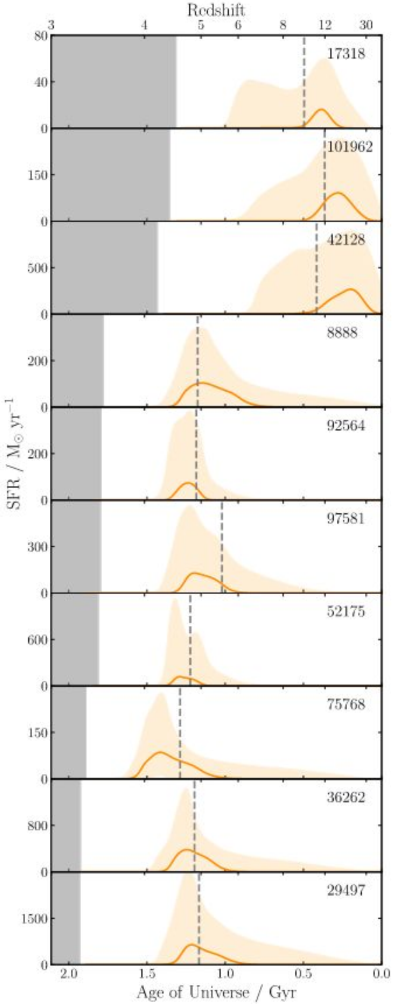

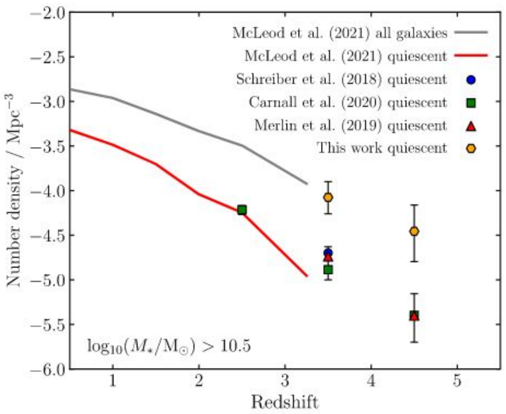

Figure 4. Number density estimates for high-redshift massive quiescent galaxies. Our estimate at $3 < z < 5$ derived from the *JWST* CEERS data are 3–5 times higher than pre-*JWST* estimates, and, at $z \simeq 3$, approach the result of McLeod et al. (2021) for the total galaxy population. Stellar masses derived by other authors have been converted to a Kroupa (2001) IMF where necessary.

Carnall+2023
EGS: 15 sources
SED-fitting selection
3<z<5, M*>1.5e10Mo
12 galaxies matched
4 objects already in EM+19
+ 8 too faint for selection

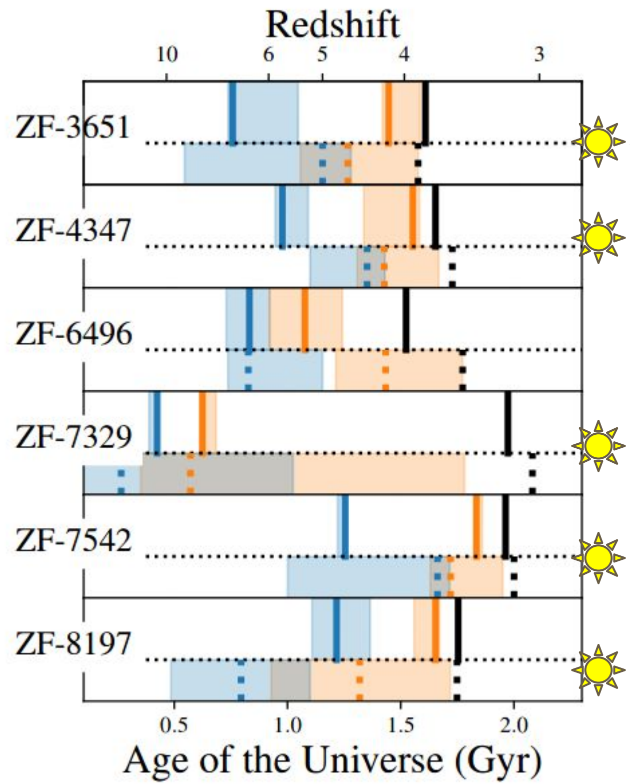

EM+19 sample

Fig. 4 The best-fit SFHS of our galaxies. The time where the galaxy formed 50% of its stellar mass is shown by the blue vertical lines and its associated $3-\sigma$ error parameterized by the FAST++ χ^2 grid is shown by the blue shaded region. The quenching time as defined by S18 (time at which the SFR of the galaxy falls below 10% of its main SFR episode, see Section 4.1 of S18 for details) is shown by the orange vertical lines with its associated error shaded in orange. The black vertical line is the age of the Universe at which the galaxy is being observed. For each galaxy, the top panels show the improved constraints obtained with our JWST/NIRSpec observations. The lower panels (below the dotted lines) show constraints reported in S18. Best-fit S18 values are shown using vertical dashed lines for clarity.

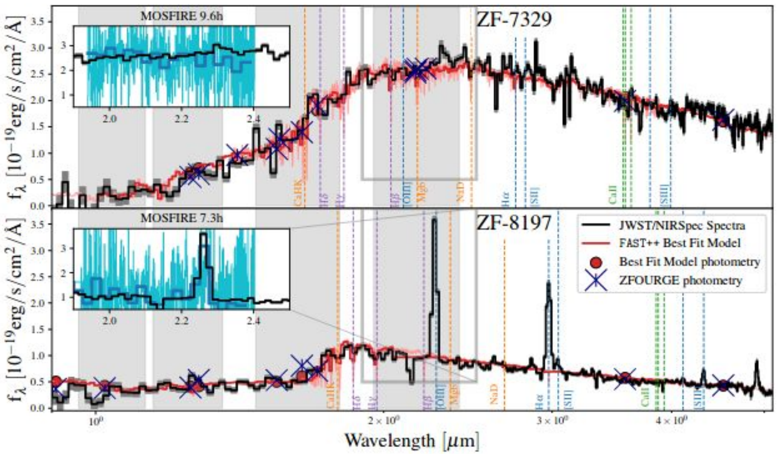

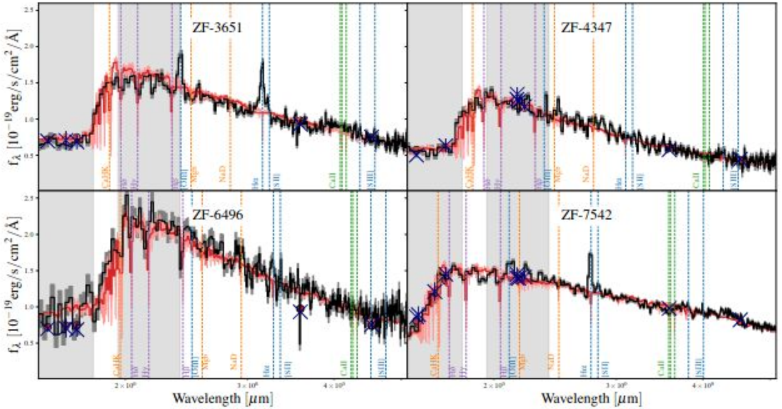

UDS, 3<z<4
Nanayakkara+2023

Spectroscopic!

A massive quiescent one at at z=4.7, quenched at 6.7

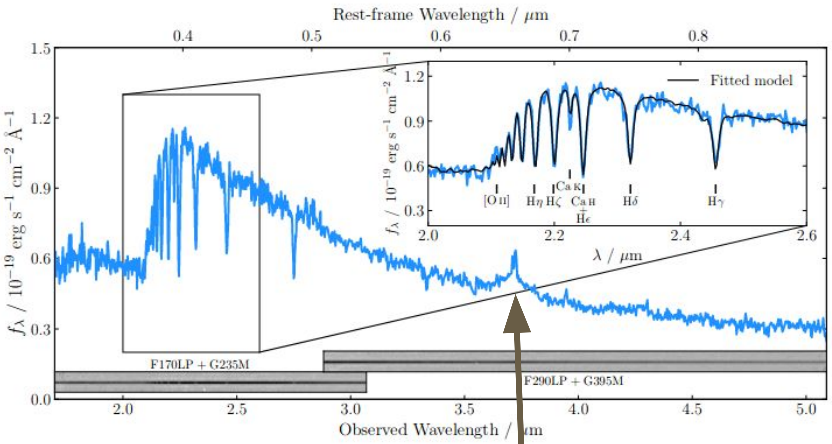

Abstract

We report the spectroscopic confirmation of a massive quiescent galaxy, GS-9209 at a new redshift record of $z = 4.658$, just **1.25** Gyr after the Big Bang, using new deep continuum observations from JWST NIRSpec. From our full-spectral-fitting analysis, we find that this galaxy formed its stellar population over a $\simeq$ **200** Myr period, approximately **600 – 800** Myr after the Big Bang ($z_{\mathrm{form}} = 7.3 \pm 0.2$), before quenching at $z_{\mathrm{quench}} = 6.7 \pm 0.3$. GS-9209 demonstrates unambiguously that massive galaxy formation was already well underway within the first billion years of cosmic history, with this object having reached a stellar mass of $\log_{10}(M_*/\mathrm{M}_\odot) > 10.3$ by $z = 7$. This galaxy also clearly demonstrates that the earliest onset of galaxy quenching was no later than $\simeq$ **800** Myr after the Big Bang.

Carnall+2023

AGN

EGS
Selected in EM+19
(non robust)

Spectroscopic!

A post-starburst at z=7.3

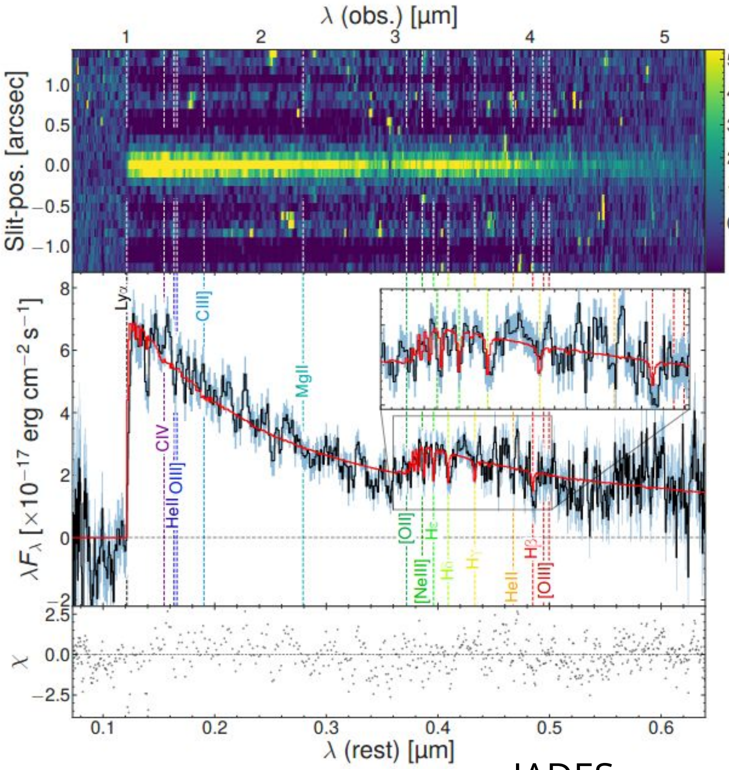

JADES, Looser+2023

Key inferred properties	PPXF	BAGPIPES	BEAGLE	PROSPECTOR
$\log_{10}(M_\star/M_\odot)$	-	8.6 ± 0.1	$8.8^{+0.1}_{-0.2}$	$8.7^{+0.1}_{-0.1}$
$\log_{10}(\mathrm{SFR}\ [M_\odot/\mathrm{yr}])$	-	< -1.3	$-2.5^{+1.0}_{-1.0}$	$-2.6^{+1.5}_{-2.7}$
$\log_{10}(Z/Z_\odot)$	< -2.0	-0.7 ± 0.1	$-1.9^{+0.4}_{-0.2}$	$-1.7^{+0.2}_{-0.2}$
t_{quench} [Myr]	~ 20	~ 10	16^{+7}_{-4}	38^{+9}_{-10}
t_{form}[Myr]	~ 100	40 ± 10	93^{+69}_{-47}	116^{+85}_{-45}
A_V [mag]	0.4 ± 0.1	$0.32^{+0.25}_{-0.17}$	$0.51^{+0.03}_{-0.04}$	$0.1^{+0.1}_{-0.0}$

“Based on colours alone, this quiescent galaxy would have been identified as ‘star forming’ if using the local and low-redshift colour selection criteria; indeed, its rest-frame U-V colour of 0.16±0.03mag places it outside the local quiescent region of the UVJ diagram, regardless of V-J colour.

Observationally, the very young age of the Universe unavoidably implies a young stellar population – even if star formation has stopped. Essentially, all quiescent galaxies in the first billion years of the Universe must be ‘post-starburst’.

Therefore, early quiescent galaxies are expected to have blue broad-band colours, very similar to the colours of star-forming galaxies, making their photometric identification challenging”

Spectroscopic!

More statistics? EUCLID

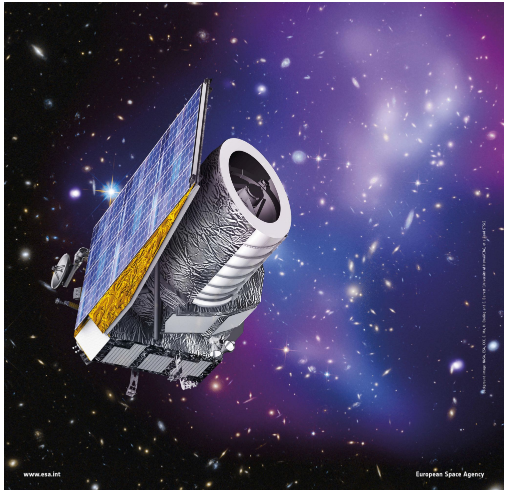

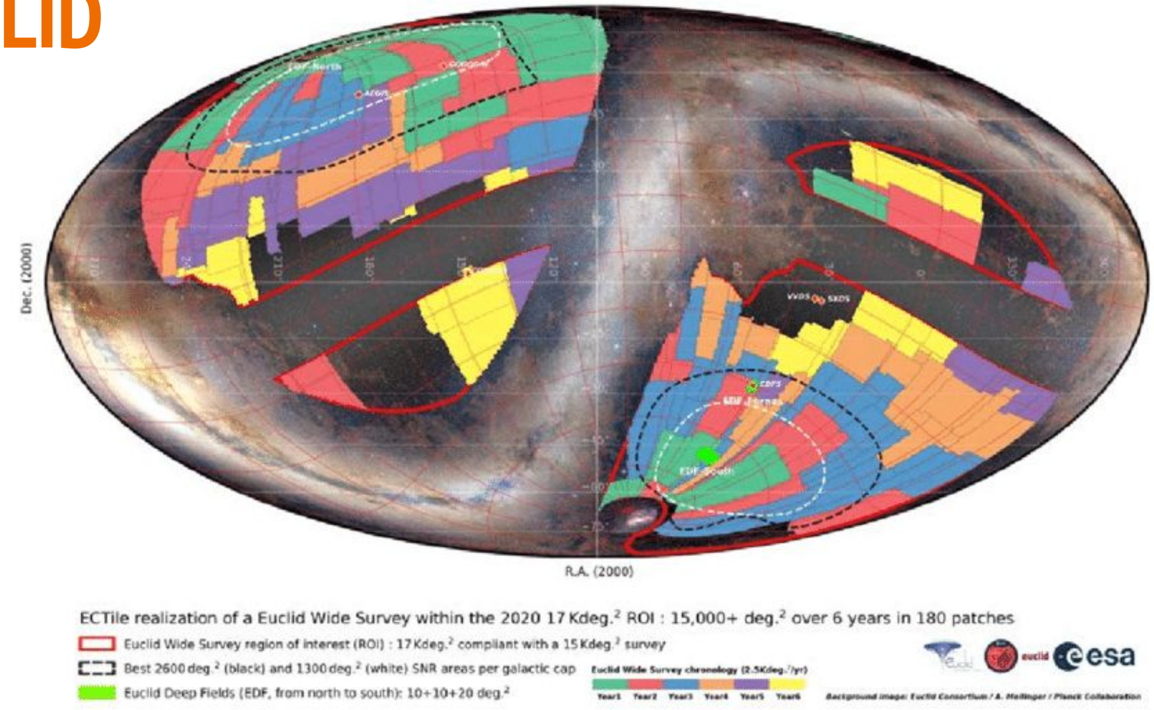

Investigates the Dark Universe via BAOs and WL

WIDE: 15000 sq deg, VIS ~ 24.5 (10σ)
1.5 billion galaxies, 600 million spectra
DEEP: 40 sq deg, VIS ~ 26.5 (10σ)
(CANDELS: ~1000 sq arcmin)
Launch in a month

EM and MC part of OU-MER:
Photometry + morphology created by automated pipelines (which we developed)
Periodic public data releases starting 6 months from launch

So, what about models?

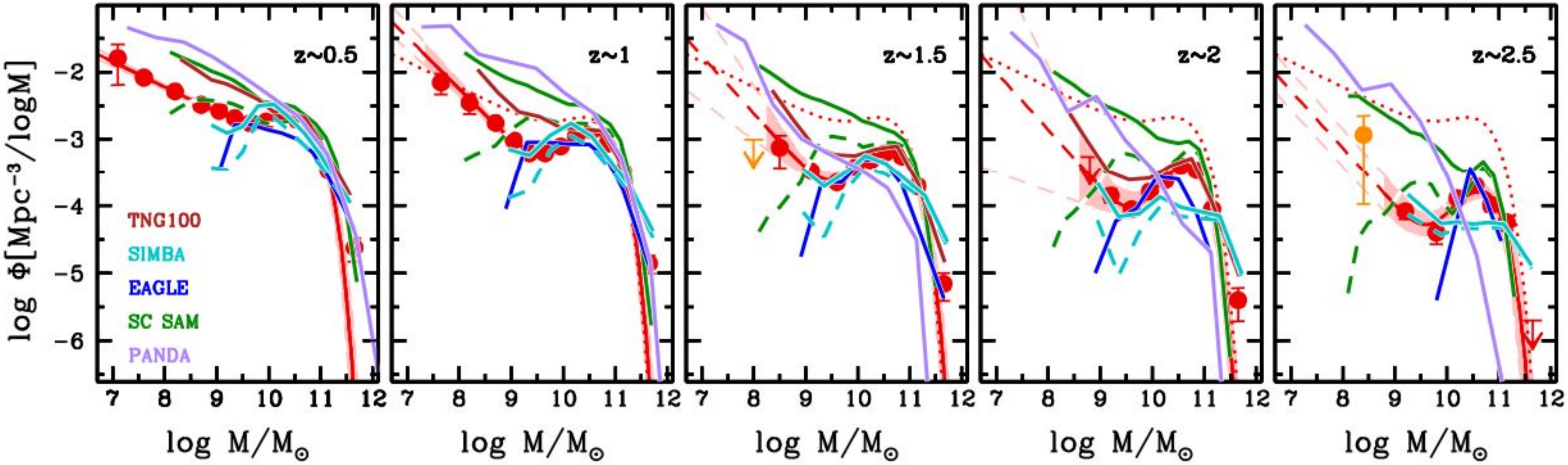

Santini+2022

3 RESULTS AND DISCUSSION: THE FIRST QUIESCENT CENTRAL GALAXIES IN TNG300

The first quiescent galaxies in TNG300 emerge at $z \sim 4.2$, roughly 1.5 Gyr after the Big Bang. No snapshots in time prior to $z = 4.18$ contain galaxies that fit our criteria. To ensure a robust selection, we experimented with a higher sSFR cut of $10^{-10}\mathrm{yr}^{-1}$, and our five selected galaxies were still the only quiescent candidates at $z = 4.18$ (with no new galaxies fitting these criteria at higher redshifts). Lowering our mass cut to $10^{10}\mathrm{M}_{\odot}$ resulted in the emergence of a new quiescent galaxy at the prior snapshot of $z = 4.43$, which was found to be a galaxy from our sample that hadn't yet reached its star formation peak. We also checked TNG50, the highest resolution simulation of the TNG suite, for galaxies meeting our original criteria, and found the first match to occur at $z = 3.0$ (mostly due to a volume effect).

Finally, we limit galaxy stellar mass M_* to $\log(\mathrm{M}_*/\mathrm{M}_{\odot}) > 10.5$. This restricts our search to subhaloes with stellar masses greater than 1000 times the baryonic mass resolution of TNG300-1, so that all galaxies are resolved with roughly 10^4 star particles.

Hartley+2023

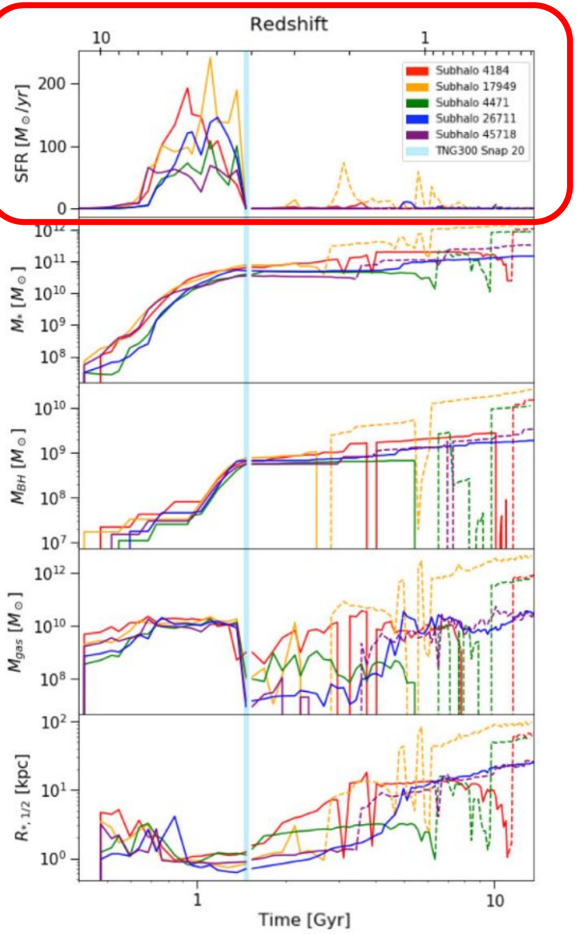

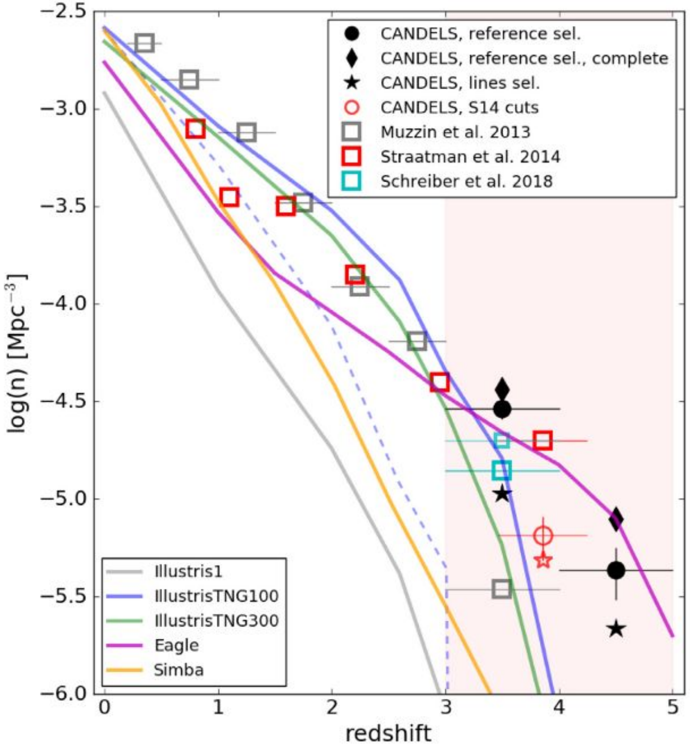

EM+2019

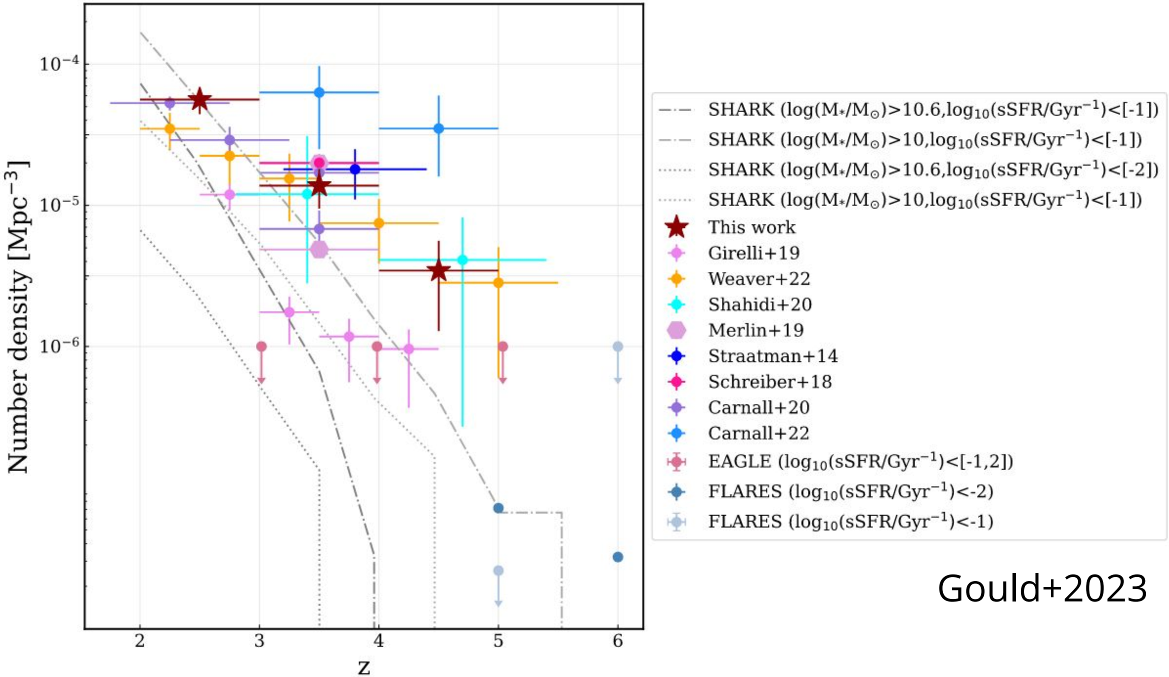

Gould+2023

Hydrodynamical structure formation in Milgromian cosmology

Nils Wittenburg[1]*, Pavel Kroupa[1,2], Indranil Banik[3,1], Graeme Candlish[4] and Nick Samaras[2]

[1] Helmholtz-Institut für Strahlen und Kernphysik (HISKP), University of Bonn, Nussallee 14–16, D-53115 Bonn, Germany
[2] Astronomical Institute, Faculty of Mathematics and Physics, Charles University, V Holešovičkách 2, CZ-180 00 Praha 8, Czech Republic
[3] Scottish Universities Physics Alliance, University of Saint Andrews, North Haugh, Saint Andrews, Fife, KY16 9SS, UK
[4] Instituto de Física y Astronomía, Universidad de Valparaíso, Gran Bretaña 1111, 2360102 Valparaíso, Chile

29 May 2023

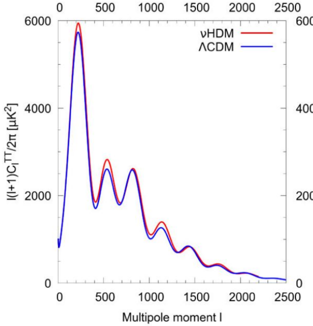

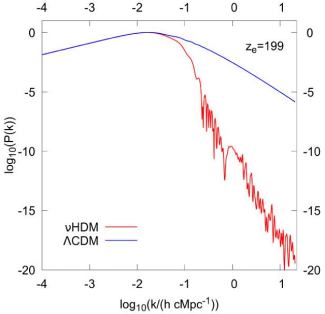

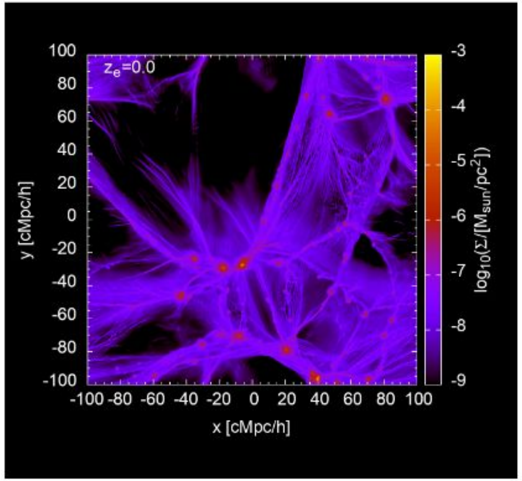

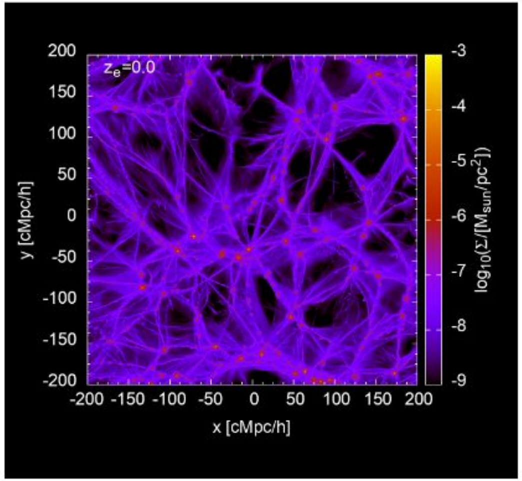

The first structures begin to form at $z_e \approx 4$ for the higher resolution simulations. This result appears to be in tension with high redshift galaxies observed with the recently launched JWST, which also seem to be in some tension with ΛCDM (Haslbauer et al. 2022a). However, previous analytic estimates of structure formation in MOND indicate that galaxy scale structures (up to $10^{11}\,M_\odot$) should have formed by $z_e = 5-10$, while cluster-sized structures ($10^{14}\,M_\odot$) should have reached maximum expansion and begun to recollapse at $z_e = 3$ (Sanders 1998). The latter is comparable to the evolution of the models shown here, but important to note is that the analytic estimates are calculated for an idealized spherical scenario without sterile neutrinos and dark energy, representing a rather different framework that may be in tension with the observed CMB. Simulations that adequately resolve galaxy mass scales (rather than just reaching this scale as we do here) are needed to conclusively test the onset of structure formation in the νHDM framework. We expect a higher resolution simulation to identify the first galaxies at earlier epochs than the structures shown here, with star formation in the first collapsing gas clouds occurring even earlier (see also Wittenburg

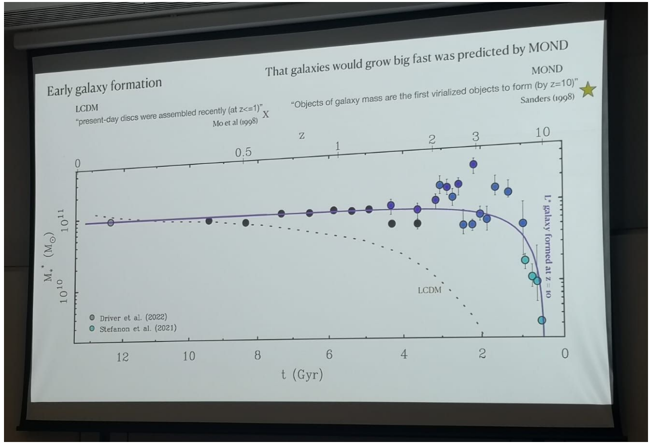

Comparing observations with models is not trivial

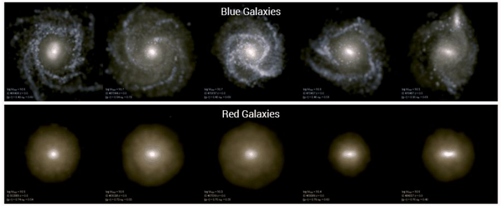

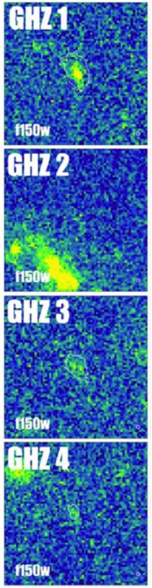

MODELS:

For all sources { Redshift, Mass, Age, Metallicity

OBSERVATIONS:

Photons

↓

Fluxes + Errors

↓

COUNTS SED

} Only for detected sources

- Incompleteness
- Assumptions
- Algorithmic limitations

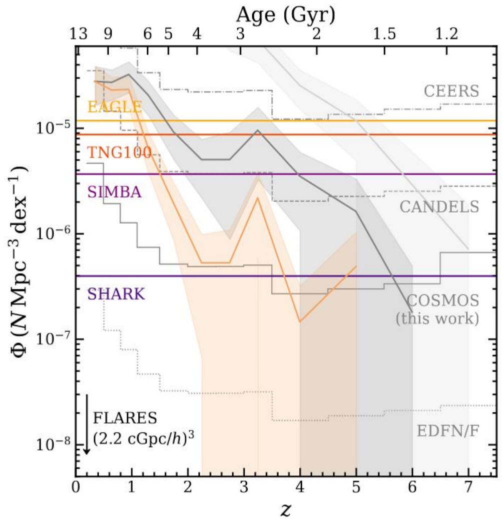

Weaver+2022

Comparing observations with models is not trivial

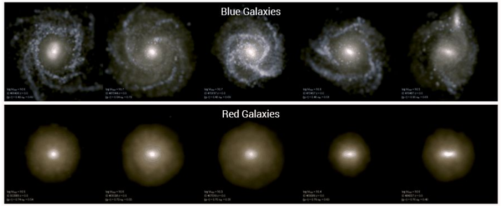

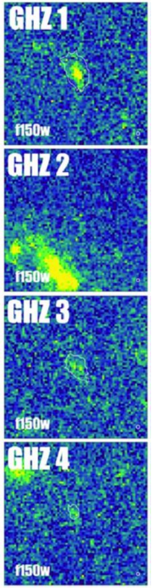

FORWARD MODELING

MODELS:

For all sources { Redshift, Mass, Age, Metallicity

↓

"true" SED

↓ Add observational sources of errors and perform measurements

COUNTS
SED

⟷

OBSERVATIONS:

Photons

↓

Fluxes
+
Errors

↓

COUNTS
SED

} Only for detected sources

FORECAST: a flexible software to forward model cosmological hydrodynamical simulations mimicking real observations

Flaminia Fortuni[1], Emiliano Merlin[1], Adriano Fontana[1], Carlo Giocoli[3,4], Erik Romelli[2], Luca Graziani[5], Paola Santini[1], Marco Castellano[1], Stéphane Charlot[6], and Jacopo Chevallard[7]

[1] INAF - Osservatorio Astronomico di Roma, via Frascati 33, 00078 Monte Porzio Catone (Roma), Italy e-mail: flaminia.fortuni@inaf.it
[2] INAF - Osservatorio Astronomico di Trieste, Via Tiepolo 11, I-34131 Trieste, Italy
[3] INFN - Sezione di Bologna, Viale Berti Pichat 6/2, 40127 Bologna, Italy
[4] INAF - Osservatorio di Astrofisica e Scienza dello Spazio di Bologna, via Gobetti 93/3, I-40129 Bologna, Italy
[5] Dipartimento di Fisica, Università di Roma "La Sapienza", Piazzale Aldo Moro 5, I-00185 Roma, Italy
[6] Sorbonne Université, CNRS, UMR 7095, Institut d'Astrophysique de Paris, 98 bis bd Arago, 75014 Paris, France
[7] Department of Physics, University of Oxford, Denys Wilkinson Building, Keble Road, Oxford OX1 3RH, UK

Received date / Accepted date

] 30 May 2023

ABSTRACT

Context. Comparing theoretical predictions to real data is crucial to properly formulate galaxy formation theories. However, this is usually done naively considering the direct output of simulations and quantities inferred from observations, which can lead to severe inconsistencies.

FORECAST

HYDRODYNAMICAL SIMULATION → particle-based FORWARD MODELING → MOCK OBSERVATORY

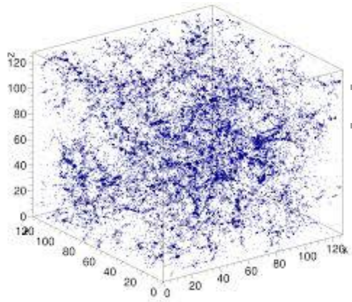

- large-volume
- full hydrodynamics

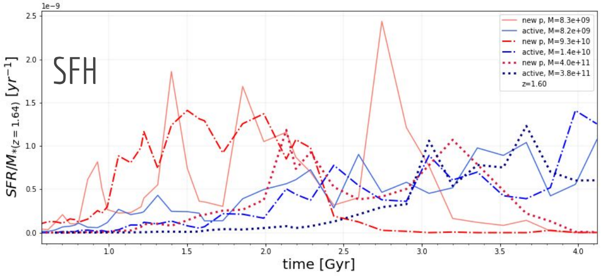

post-processing of the simulation:

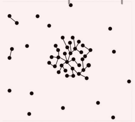

stellar particles as galaxy tracer
gas cells as dust tracer

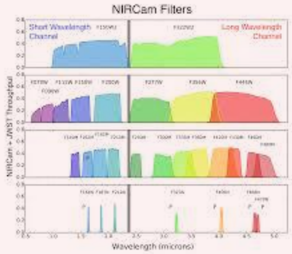

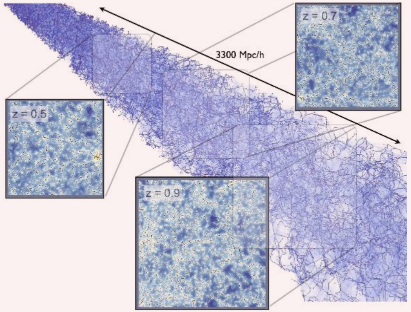

imaging from rest-frame **ultraviolet** to **near-infrared** bands

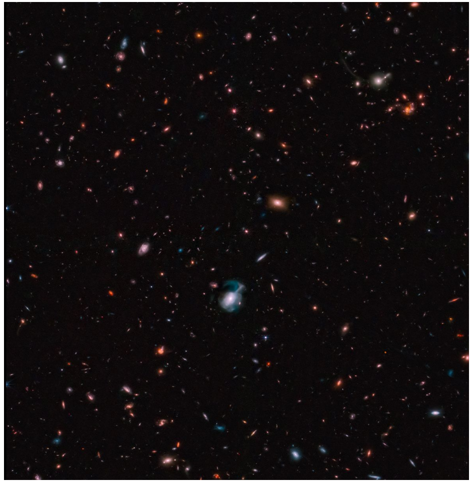

crop of *JWST*/CEERS
Credits: https://ceers.github.io/

Testing FORECAST emulating the CANDELS GOODS-South field

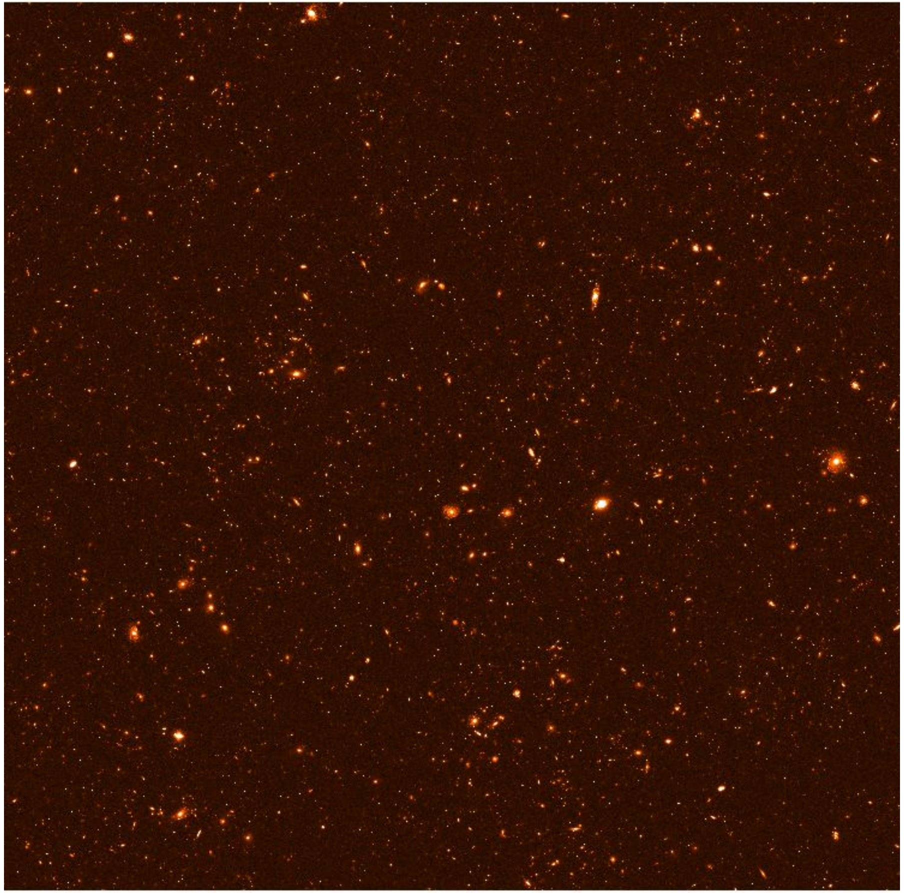

Final simulated light-cone in H160 band (PSF and noise added in post-processing)

light-cone between $0.1 \leq z \leq 7.0$
field of view 200 arcmin^2, with pixel scale 0.06 arcsec

ASTRODEEP catalogue from **CANDELS GOODS-South field** (Merlin+2021) exploiting **IllustrisTNG-100** (Weinberg+2017, Pillepich+2018)

post-processing:

- instrumental PSF + bkg gaussian noise + shot noise
- RMS map

Testing FORECAST emulating the CANDELS GOODS-South field

ACS B435	WFC3 Y105	WFC3 H160	IRAC CH1

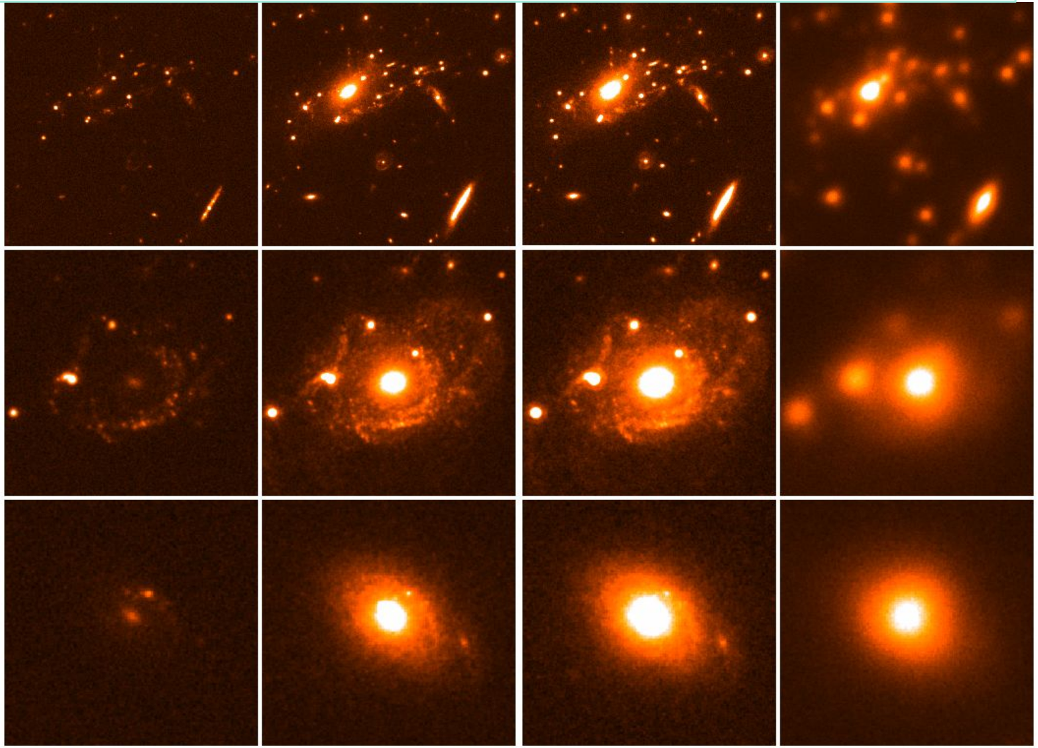

Example of small areas containing a group and single objects, in 4 simulated bands (in μJy; light-cone with PSF and noise added in post-processing)

JWST mock dataset

WFC3 f160w

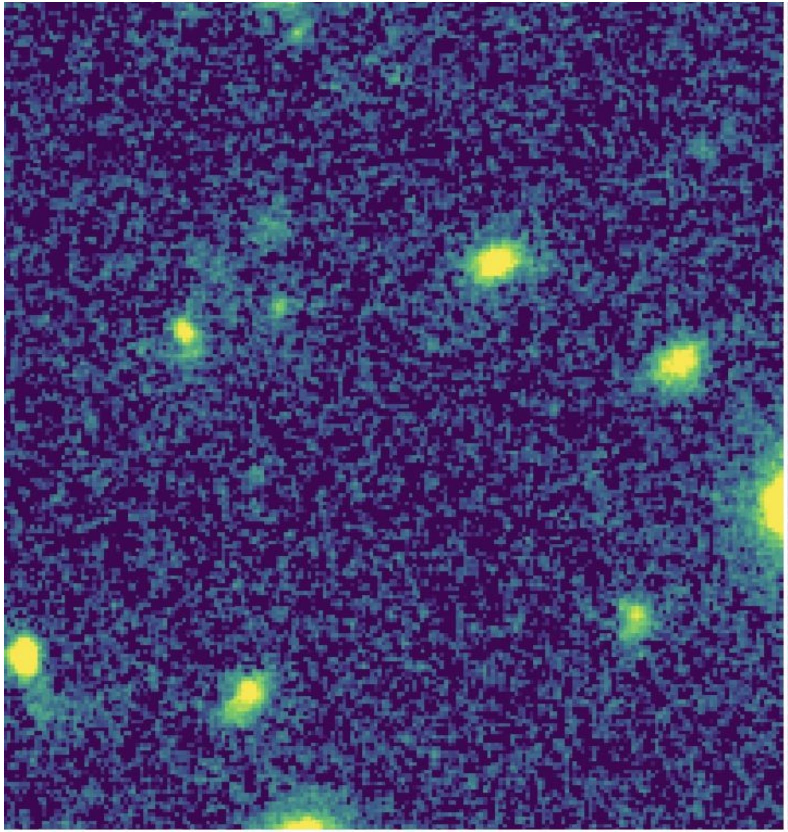

NIRCam f150w

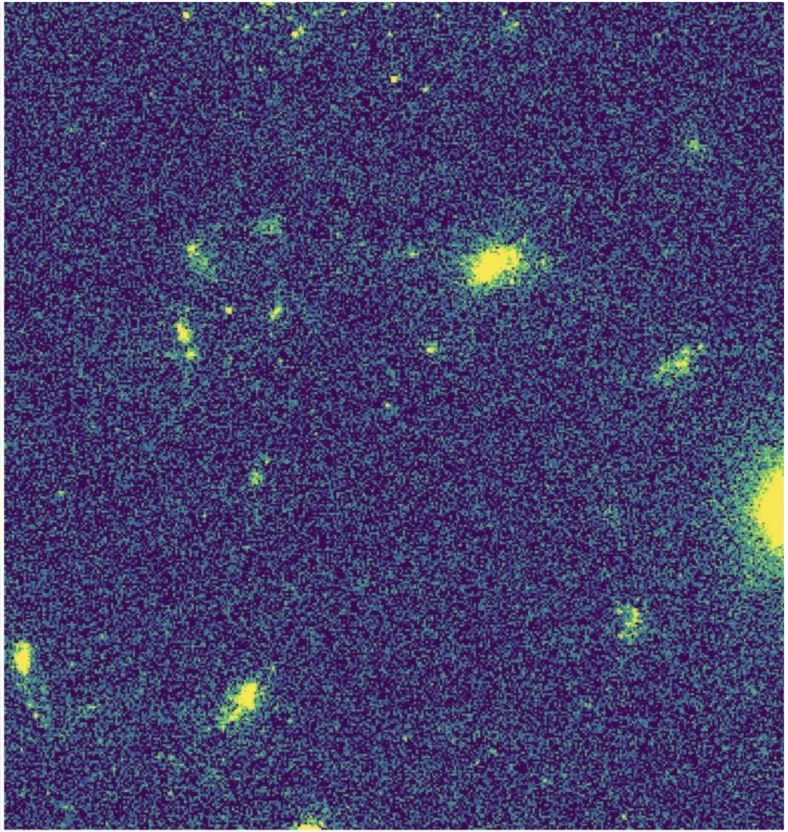

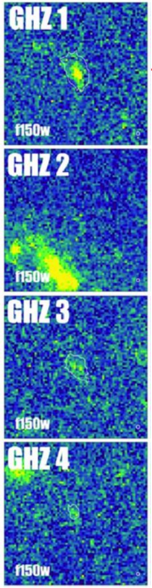

SED-fitting tests: photometric redshift

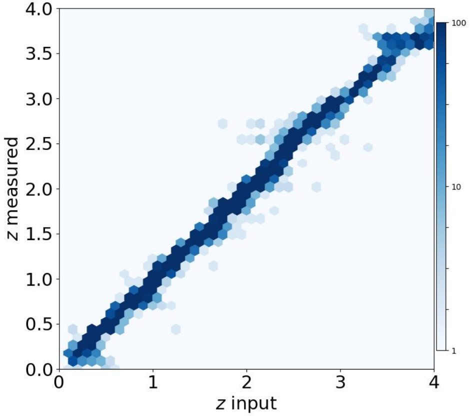

input photometry

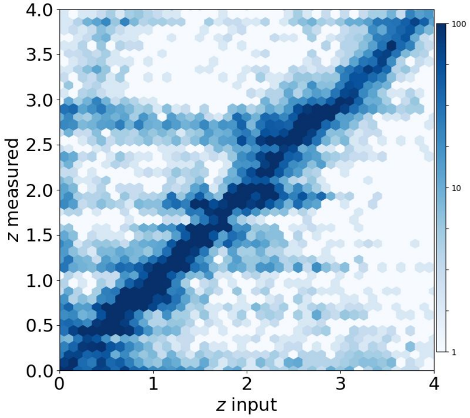

measured photometry

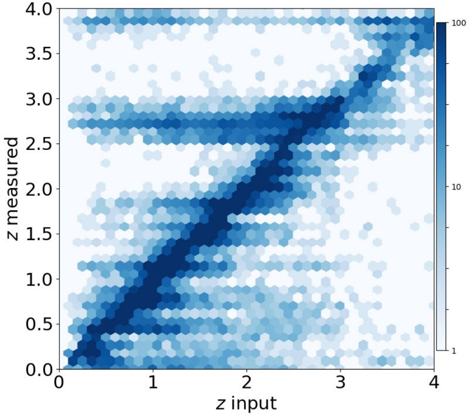

REAL WORLD:
GOODS-South field

SED-fitting tests: stellar masses

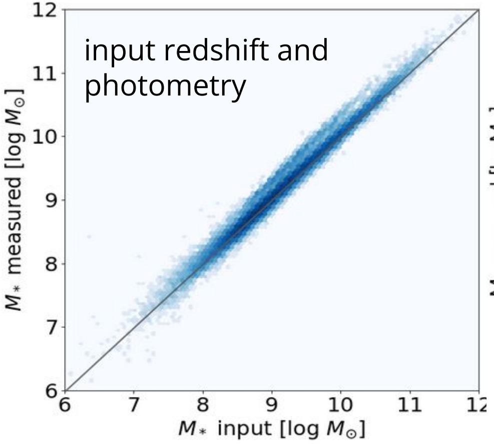

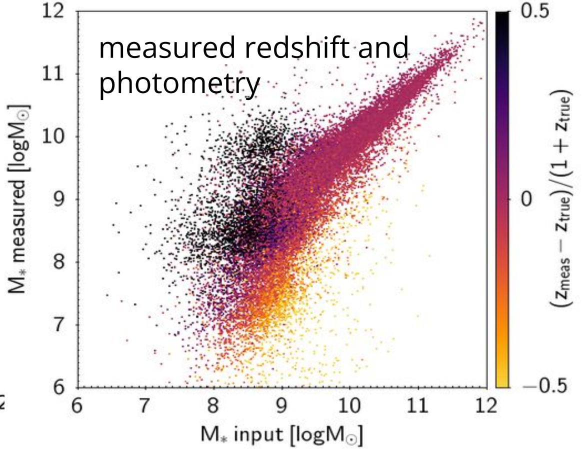

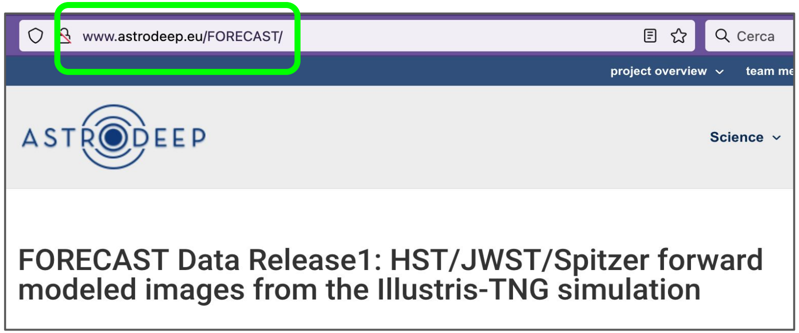

CONCLUSIONS

Massive, passive galaxies are confirmed at z>4, detected at z~5 and beyond

While photometric selection can be problematic at z>5, JWST spectra provide the first evidences of the existence of QGs at z~6-7

Euclid will soon provide tons of data

These objects challenge LCDM: models do not produce them

Waiting for MOND-ian predictions!

Models and observations shall be compared properly: forward-modeling (FORECAST)

Question: are there tests of MOND that can be performed with (photometric) data of high-z (passive) galaxies?

Thanks!

emiliano.merlin@inaf.it
astrodeep.eu

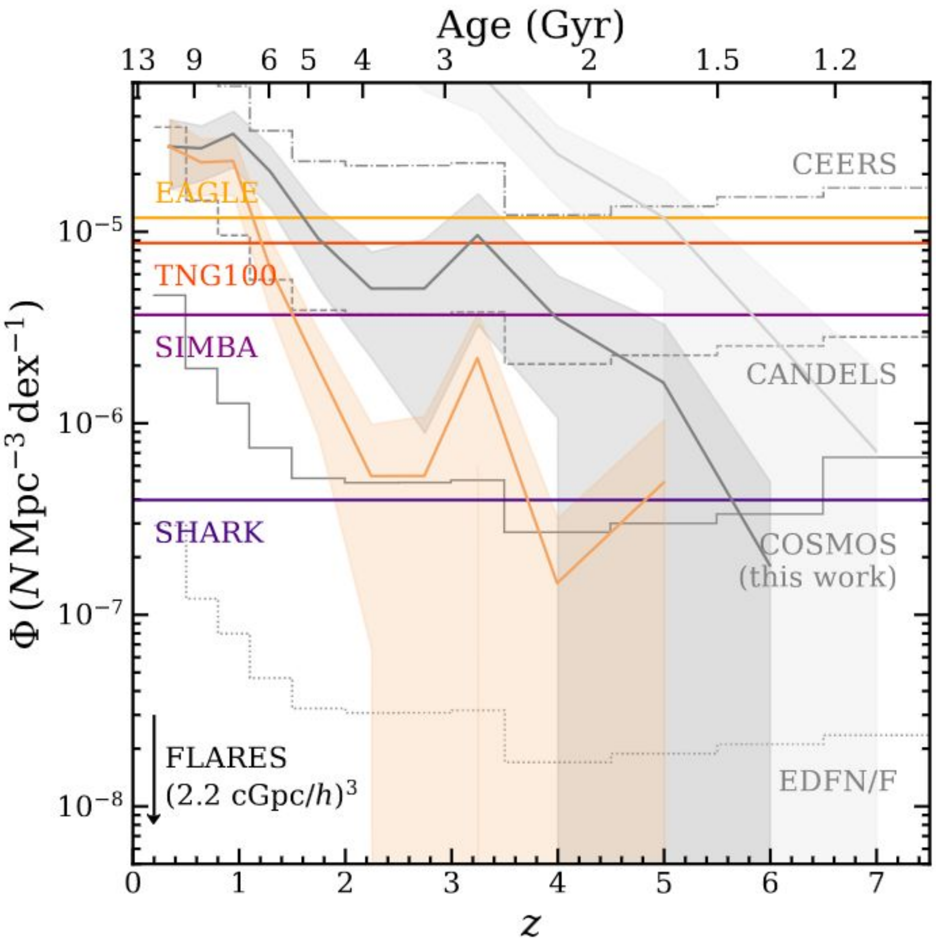
Age (Gyr)
13
9
6
5
4
3
2
1.5
1.2
CEERS
EAGLE
TNG100
SIMBA
CANDELS
SHARK
COSMOS
(this work)
EDFN/F
FLARES
(2.2 cGpc/h)^3
10^{-5}
10^{-6}
10^{-7}
10^{-8}
$\Phi\,(N\,\mathrm{Mpc}^{-3}\,\mathrm{dex}^{-1})$
0
1
2
3
4
5
6
7
z

Weaver+2022

A massive dead galaxy at *z*=6.7?

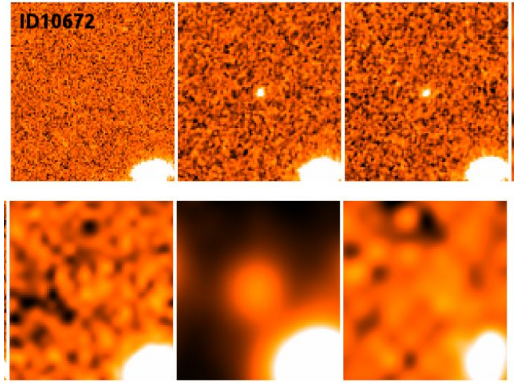

z_{form} ~ 14

SFR_{burst} ~ 130 M_{sol}/yr

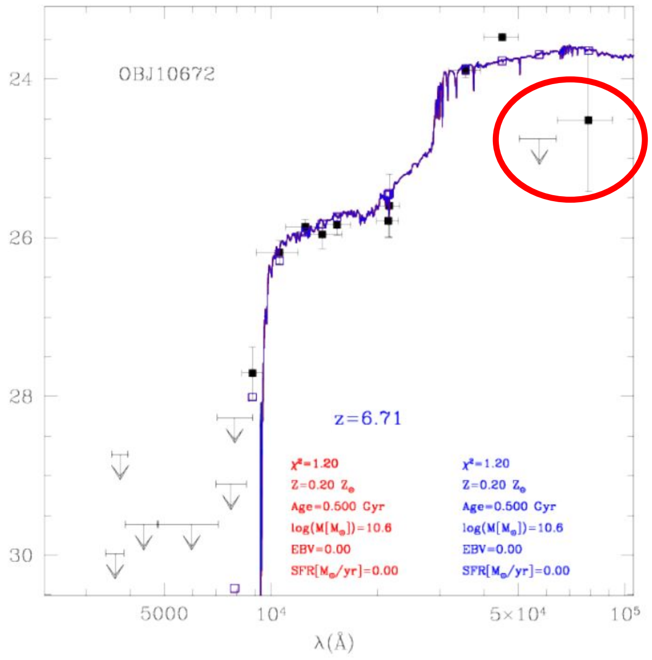

Merlin+19

- No detectable flux in *Herschel*
- Catalogued in many surveys (e.g. Finkelstein+2015; Bouwens+2015; Harikane+2016) as a *z* ~ 6 – 7 mildly star forming or quiescent galaxy
- Classified as a *z* = 1.73 source in 3D-HST by means of EAzY photo-*z* estimate
- Might be a cold brown dwarf?

> Too faint for spectroscopic analysis with current facilities; *J* band continuum might be visible with MOSAIC (S/N=5 in 4~5 hrs - MOSAIC white paper)

Spectroscopic confirmations at z 3-4

Karl Glazebrook[1], Corentin Schreiber[2], Ivo Labbé[2], Themiya Nanayakkara[1], Glenn G. Kacprzak[1] Pascal A. Oesch[3], Casey Papovich[4], Lee R Spitler[5,6], Caroline M. S. Straatman[7], Kim-Vy H. Tran[4], Tiantian Yuan[8]

retical models.[7-10] Here, we report the spectroscopic confirmation of one of these galaxies at redshift z=3.717 with a stellar mass of 1.7×10^{11} $M_\odot$ whose absorption line spectrum shows no current star-formation and which has a derived age of nearly half the age of the Universe at this redshift. The observations demonstrates

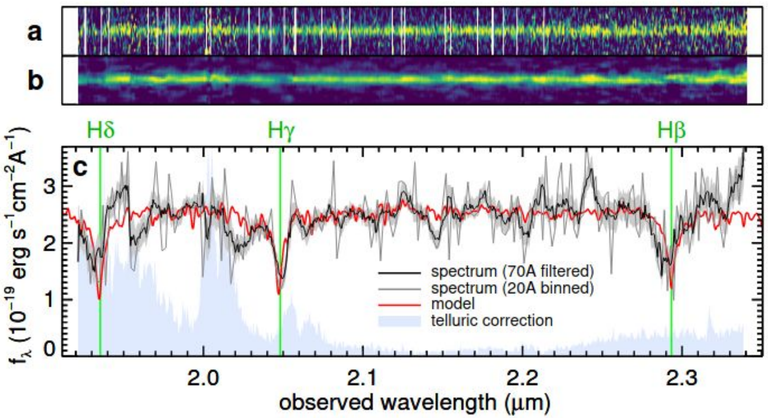

Originally published in 2017
Included in EM+19
See also Schreiber+2018 "Jekyll & Hyde"

2020

The Massive Ancient Galaxies at $z > 3$ NEar-infrared (MAGAZ3NE) Survey: Confirmation of Extremely Rapid Star Formation and Quenching Timescales for Massive Galaxies in the Early Universe*

Ben Forrest[1], Z. Cemile Marsan[2], Marianna Annunziatella[3,4], Gillian Wilson[1], Adam Muzzin[2], Danilo Marchesini[3], M. C. Cooper[5], Jeffrey C. C. Chan[1], Ian McConachie[1], Percy Gomez[6], Erin Kado-Fong[7], Francesco La Barbera[8], Daniel Lange-Vagle[3], Julie Nantais[9], Mario Nonino[10], Paolo Saracco[11], Mauro Stefanon[12], and Remco F. J. van der Burg[13]

UMG	z_{phot}	z_{spec}	$\log(M_{*,phot}/M_\odot)$	$\log(M_{*,spec}/M_\odot)$
COS-DR3-202019	$3.10^{+0.06}_{-0.04}$	$3.1326^{+0.0021}_{-0.0011}$	$11.52^{+0.02}_{-0.04}$	$11.67^{+0.04}_{-0.05}$
XMM-VID3-2293	$3.07^{+0.17}_{-0.16}$	$3.3132^{+0.0009}_{-0.0007}$	$11.56^{+0.03}_{-0.05}$	$11.57^{+0.02}_{-0.05}$
XMM-VID1-2075	$3.48^{+0.08}_{-0.07}$	$3.4520^{+0.0014}_{-0.0017}$	$11.49^{+0.02}_{-0.03}$	$11.52^{+0.00}_{-0.05}$
XMM-VID3-1120	$3.40^{+0.12}_{-0.10}$	$3.4919^{+0.0018}_{-0.0029}$	$11.44^{+0.03}_{-0.04}$	$11.47^{+0.02}_{-0.03}$
COS-DR3-160748	$3.35^{+0.02}_{-0.09}$	$3.3524^{+0.0008}_{-0.0006}$	$11.47^{+0.03}_{-0.03}$	$11.46^{+0.01}_{-0.08}$
COS-DR3-201999	$3.14^{+0.09}_{-0.09}$	$3.1313^{+0.0014}_{-0.0012}$	$11.40^{+0.02}_{-0.05}$	$11.40^{+0.03}_{-0.01}$
COS-DR3-179370	$3.14^{+0.72}_{-0.28}$	$3.3673^{+0.0010}_{-0.0007}$	$11.34^{+0.05}_{-0.02}$	$11.37^{+0.04}_{-0.07}$
COS-DR3-195616	$3.09^{+0.09}_{-0.08}$	$3.2552^{+0.0012}_{-0.0009}$	$11.31^{+0.03}_{-0.03}$	$11.31^{+0.02}_{-0.02}$
COS-DR3-208070	$3.44^{+0.06}_{-0.05}$	$3.4912^{+0.0011}_{-0.0012}$	$11.27^{+0.02}_{-0.10}$	$11.26^{+0.04}_{-0.04}$
XMM-VID3-2457	$3.51^{+0.07}_{-0.07}$	$3.4892^{+0.0032}_{-0.0024}$	$11.20^{+0.03}_{-0.01}$	$11.26^{+0.02}_{-0.03}$
COS-DR3-84674	$3.06^{+0.06}_{-0.06}$	$3.0094^{+0.0015}_{-0.0011}$	$11.26^{+0.02}_{-0.04}$	$11.25^{+0.01}_{-0.02}$
COS-DR1-113684	$3.47^{+0.08}_{-0.08}$	$3.8309^{+0.0014}_{-0.0020}$	$11.20^{+0.04}_{-0.06}$	$11.20^{+0.03}_{-0.04}$
COS-DR3-131925	$3.20^{+0.08}_{-0.08}$	$3.1393^{+0.0008}_{-0.0013}$	$11.17^{+0.04}_{-0.02}$	$11.12^{+0.12}_{-0.05}$
COS-DR3-226441	$3.27^{+0.06}_{-0.06}$	$3.2446^{+0.0014}_{-0.0012}$	$11.34^{+0.02}_{-0.03}$	$11.02^{+0.06}_{-0.03}$
XMM-VID1-2399	$3.68^{+0.11}_{-0.12}$	$3.5798^{+0.0010}_{-0.0009}$	$11.18^{+0.08}_{-0.09}$	$11.02^{+0.14}_{-0.13}$
COS-DR3-111740	$3.12^{+0.05}_{-0.06}$	$2.7988^{+0.0013}_{-0.0011}$	$11.13^{+0.03}_{-0.04}$	$10.98^{+0.01}_{-0.00}$

Analysis of spectroscopic data available at the time supported the passive nature of candidates

Herschel and ALMA confirmations

Santini+2019,2021

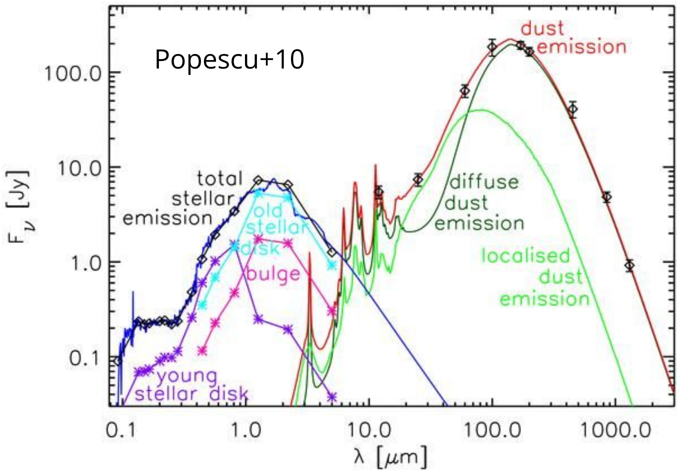

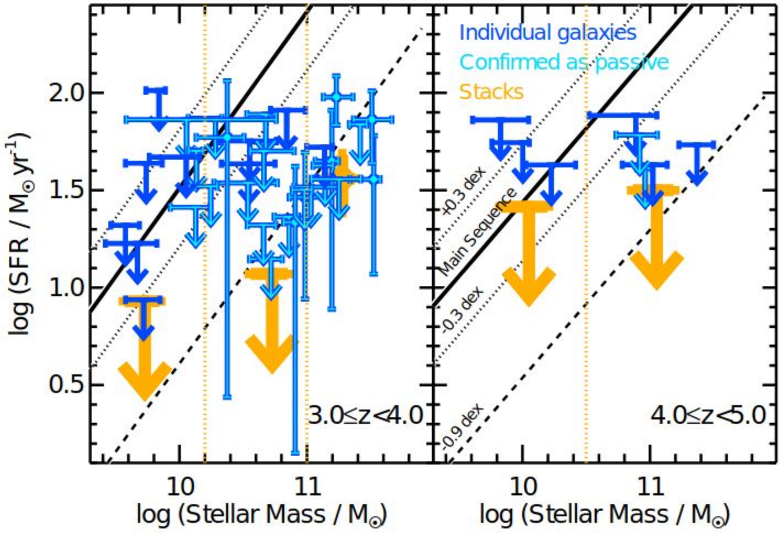

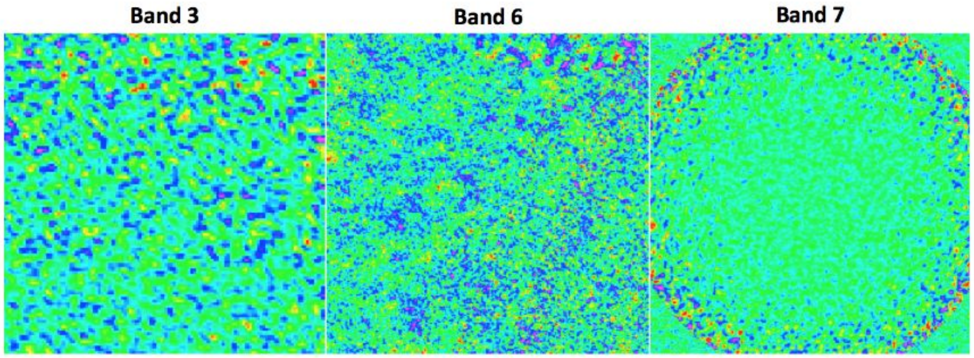

Figure 1. Stacked continuum images in Band 3, 6 and 7, of 2, 20 and 9 sources, respectively, from left to right.

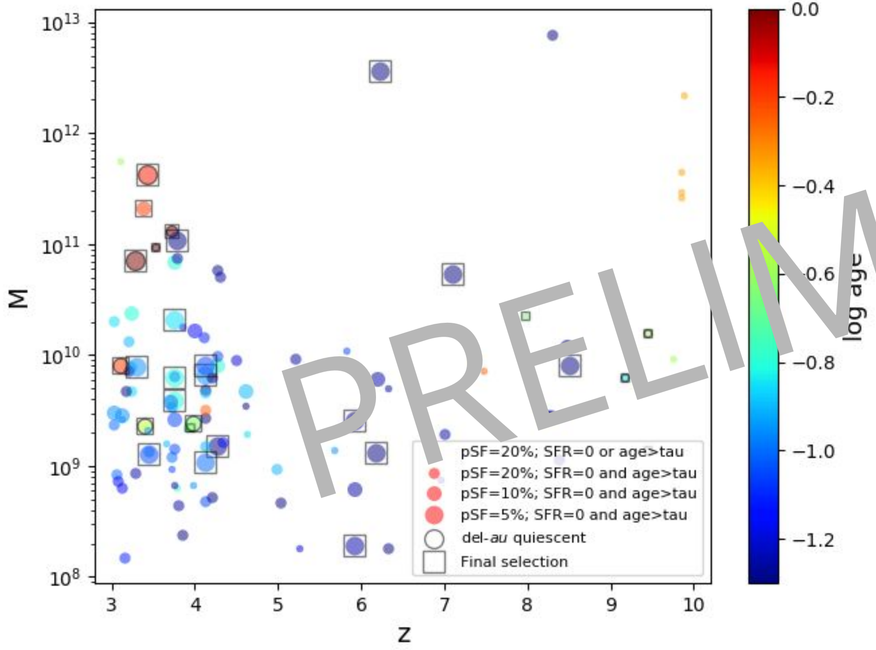

Abell2744

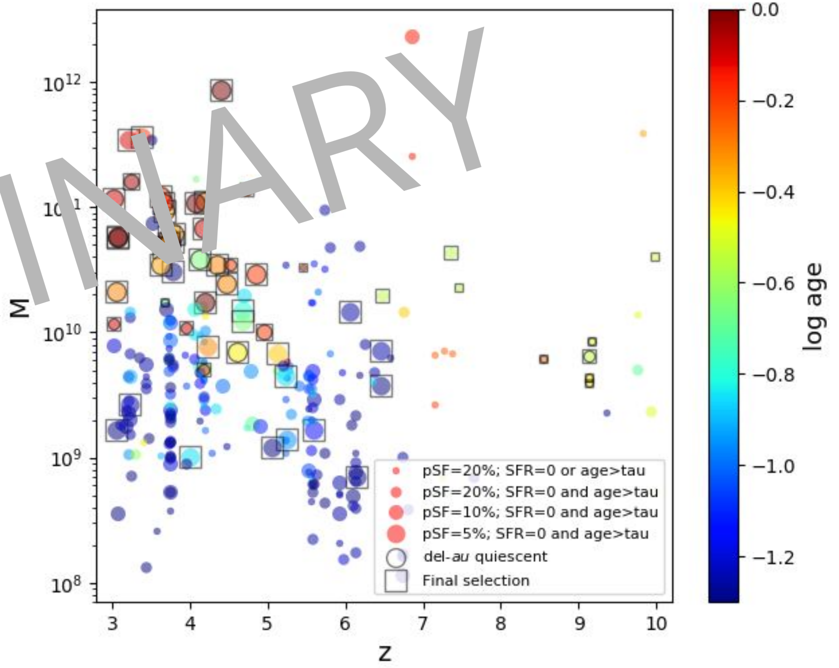

EGS (CEERS)

Adding COSMOS and UDS (PRIMER), GOODS N+S (JADES), NGDEEP